University POLITEHNICA București

Faculty of Aerospace Engineering

Aerospace Engineering Doctoral School

Ph.D.THESIS SUMMARY

Contributions regarding the study of axial turbines stability and performance enhancement

Contribuții privind studiul stabilității și menținerii performanțelor turbinelor axiale

Author: Eng. Răzvan NICOARĂ

PhD supervisor: Eng., PhD, Prof. Daniel CRUNȚEANU

Bucharest, 2023

CUPRINS

CHAPTER 1 - DOCTORAL THESIS MOTIVATION AND OBJECTIVES

General considerations

Aircraft propulsion is largely achieved through the use of gas turbine engines due to the multiple advantages of these systems such as: high powers relative to the mass of the system, reliability, low maintenance costs, high performance over a wide range of altitudes and speeds, etc. The uses of gas turbine engines are not limited to the aeronautical industry, due to the previously mentioned advantages they have been and are successfully used in other industries such as: land and marine propulsion, electricity generation, gas pumping, fire fighting, etc.

Modern gas turbine engines must ensure high performance and specific fuel consumptions as low as possible while ensuring efficient operation over a wide range of regimes and operating conditions. Over time, the increase gas turbine engines performance was possible both through the individual optimization of the components (compressor, combustion chamber and turbine) but especially through the optimization of the thermodynamic cycle, consisting in the increase of working temperatures and pressures. These increases have been made possible by technological advances in related fields such as materials technology, combustion, channel flows, heat and mass transfer, etc.

A study of part loads in the 25-100% range on a single-rotor structure illustrates their influence on compressor and turbine efficiency. (1) For each regime, the temperature at the turbine inlet was determined, the variation being presented in Figure 1.1. A strong drop in turbine efficiency can be observed at low speeds, the performance of the turbine being strongly affected by the drop in temperature at the exit from the combustion chamber.

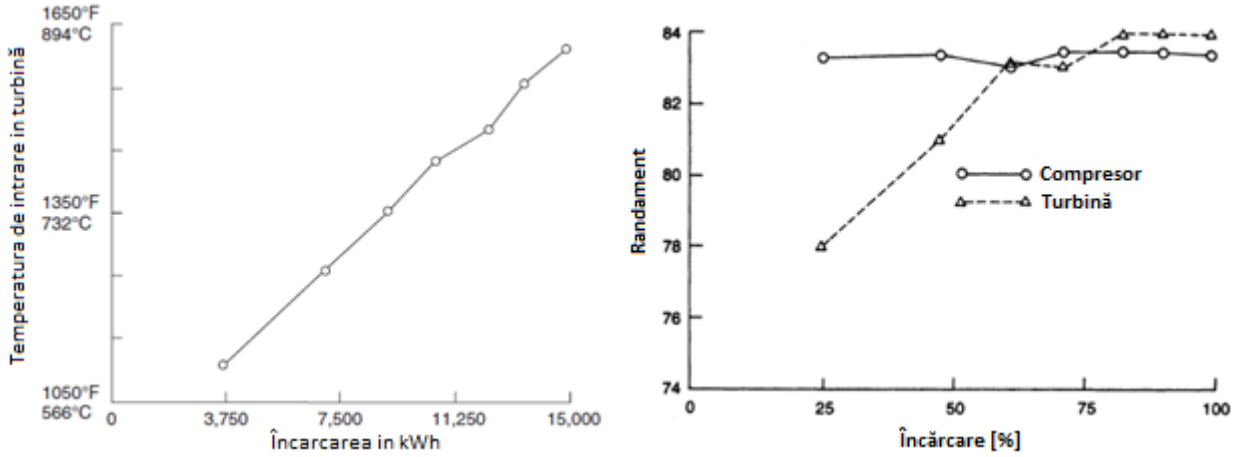

Figure 1.1. Temperature and efficiency variation as a function of partial loads (1)

In the case of aviation gas turbine engines, operation at partial regimes is encountered when the aircraft is taxiing to the runway or to the parking area, when the aircraft is stopped on the runway with the engines operating at idle speed, but also in flight during the descent procedure and landing. Higher partial loads may also be encountered during flight depending on

flight conditions and fuel consumption requirements. In these cases, when the engine speed is low, the performance decrease significantly. If for the case of partial regimes in flight (descent or landing) the lower performances mainly affect fuel consumption, in the case of partial regimes encountered on the ground the main problem is the resulting pollution. As a result of the increase in air traffic and the number of flights, the waiting times for take-off have increased, thus the engines operate at idle for a longer period, a regime in which their efficiency is low, resulting in increased pollution in an intensively populated area.

For gas turbine engines used in marine propulsion operation at partial regimes is common, in the case of cruise engines these regimes can be maintained for long time intervals (tens of hours). Thus, the specific consumption for these regimes is high. A similar case is found in gas turbine engines used for land propulsion, where operation at partial regimes is common.

Motivation and objectives

As mentioned earlier, gas turbine engines are widely used in various industries and this is expected to increase in the future. Operation of these systems at regimes different from those for which they were designed causes a decrease in performance which leads to an increase in specific fuel consumption and pollution. One cause of this decrease is the deterioration of turbine performance caused mainly by changing inlet parameters.

It is thus possible to identify a less studied shortcoming of these engines and respective turbines, namely the low performance for operation at regimes other than the nominal one. The general objective of this paper is to study the decrease in performance of the axial turbines and to identify a method to mitigate these shortcomings.

Thesis structure

In order to fulfil the general objective and the specific objectives, the doctoral thesis ***"Contributions regarding the study of axial turbines stability and performance enhancement"*** is divided into 9 chapters to which annexes and bibliography are added, as follows:

- **Chapter 1**, named "***Doctoral thesis motivation and objectives*** ", highlights the reasons that led to the start of scientific studies in this direction, namely the need to improve the performance of gas turbine engines at partial regimes by improving the performance of axial turbines at low loads. Also, in this chapter, the performance study of axial turbines and the methods of mitigating their decrease at partial regimes is mentioned as the general objective of the thesis.
- **Chapter 2**, called "***State of the art in the field of axial gas turbines***" presents a study of the gas turbines currently used in terms of their performance. Through this study, the identification of existing performances and solutions was sought, thus motivating the need for the research undertaken in the present work.

- **Chapter 3**, entitled "***Mathematical model for determining the performance of axial turbines***" presents the fundamental principles of fluid expansion in axial turbine channels as well as the flow characteristics at partial regimes.
- **Chapter 4**, entitled "***Research methodology of the flow control method in the bladed channels of axial turbines***" proposes a method of increasing the performance of axial turbines at partial regimes by fluid injection as well as a research methodology of the proposed system.
- **Chapter 5**, entitled "***Numerical study regarding the method of increasing performance through fluid injection - 2D model***" presents the study carried out according to the previously proposed research methodology to determine the influence of different geometrical parameters (e.g. injection angle, orifice diameter, axial positioning) as well as gas dynamics parameters (e.g. injection fluid temperature and mass flow rate). The study is carried out on a simplified 2D model representative of the mean radius of the reference turbine.
- **Chapter 6**, entitled "***Numerical study regarding the method of increasing performance by fluid injection - 3D model***" presents the continuation of the study according to the proposed methodology by determining the influence of the specific geometric parameters for the three-dimensional model (e.g. the number of orifices). Also within this chapter, the methodology for generating the injection system is established, mentioning the steps for generating the numerical model of the stator that has the injection system in its composition, as well as determining the influence of the injection system for different partial regimes.
- **Chapter 7**, entitled "***Verification of the performance improvement method of axial turbines at partial regimes***" presents a verification of the results obtained by applying the performance improvement method for other turbine geometries, with different sizes, at different partial regimes.
- **Chapter 8**, entitled "***Determining the reaction of the engine assembly to the activation of the injection system***" presents the analysis of the injection system influence on the gas turbine engine regimes and on the other components of the assembly. The analysis determines the stabilized regime after the injection and the processes necessary to return to the initial regime.
- **Chapter 9**, named "***Final conclusions, original contributions and future perspectives***" presents the final conclusions of the paper, mentioning the original contributions in relation to the current state of development in the field of gas turbines as well as future research directions for the implementation of the proposed system .

CHAPTER 2 - STATE OF THE ART IN THE FIELD OF AXIAL GAS TURBINES

The history of the development of axial turbines is closely related to the development of gas turbine aviation engines. In 1944, the Junkers Jumo 004 engine entered series production

marking the beginning of use of gas turbine engines and implicitly gas turbines in aviation, it also marked the beginning of the decline of piston engines in this industry. Due to the requirements imposed on aviation engines, the development of turbines continued in the direction of obtaining high powers using a reduced number of stages (high loading per stage) and increasing efficiency. Modern axial turbines used in aviation engines have reached a high technological level; the working fluids leaving the combustion chamber can have temperatures of up to 1700 °C, well above the melting temperature of the turbine materials (2). In these extreme conditions, the turbine operate with high efficiency even if they are subjected to enormous centrifugal forces, due to high revolutions, and to torsion forces resulting from the change in the direction of the working fluids. The evolution of turbines is also visible in terms of their resource. If the first axial turbines used in aviation engines had a low resource of several tens of hours, mainly due to the materials used, today the resource of turbines is equal to that of engines, being able to reach values of 30,000 hours.

General aspects

A schematic diagram of an axial gas turbine is shown in Figure 2.1 showing a section through a 3-stage turbine (Figure 2.1A) and a section through a single turbine stage (Figure 2.1B). In this scheme, the notation "3T" was used to symbolize the inlet to the turbine, respectively "4T" for the exit from the axial turbine.

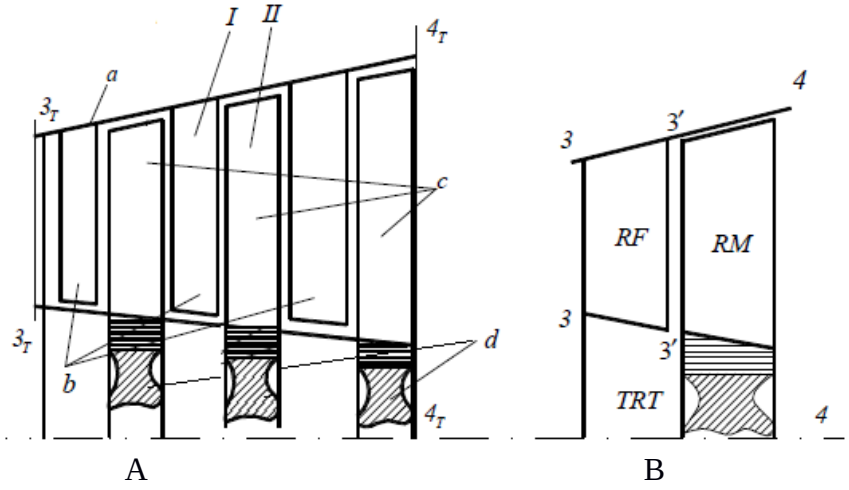

Figure 2.1. Axial turbine scheme with: A - 3 stages, B – single stage

Following the combustion process, due to the released heat, the potential energy of the fluid increases greatly while the kinetic energy remains low due to the low velocities at the exit from the combustion chamber. Thus, in order to extract energy from the working fluid and transmit it further, to the compressor or any other consumer, the turbine transforms the potential energy into kinetic energy (in the fixed channels) and then into mechanical work (in the mobile blades).

If the preliminary design is done at the mean radius of the vane, by establishing the velocity triangles, it is necessary to add the radial component for profiling the blades. In the case of turbines with small blade heights, the variations of the parameters on the radius are not significant, in this case the use of cylindrical blades is preferred (for technological reasons), while for the last stages of a power turbine, for example, where the height of the blades is significant, the mean radius analysis cannot be assumed to be representative of distant sections. Thus, in the sections at the base, top and a number of intermediate sections, the velocity triangles are established according to a profiling law

Axial turbines performance

The turbine, being a main component of gas turbine engines, has been the subject of numerous studies in order to improve performance. Various methods of designing and optimizing turbine stages have been developed over time. The introduction of numerical methods and CFD (Computational Fluid Dynamics) simulations allowed a better prediction of the flow through networks by solving the flow equations in all directions, thus including the flow in the radial direction.

The performance of the turbine, determined theoretically or experimentally, is presented in the form of characteristics. Figure 2.2 shows the power characteristic of an axial stage theoretically obtained using CFD numerical calculation. The determination of the characteristics based on the CFD numerical calculation was described in (3) and (4). It can be observed that for a decrease in inlet conditions (reduced flow) the power developed by the turbine, expressed in the form of the specific enthalpy variation, has a strong decrease.

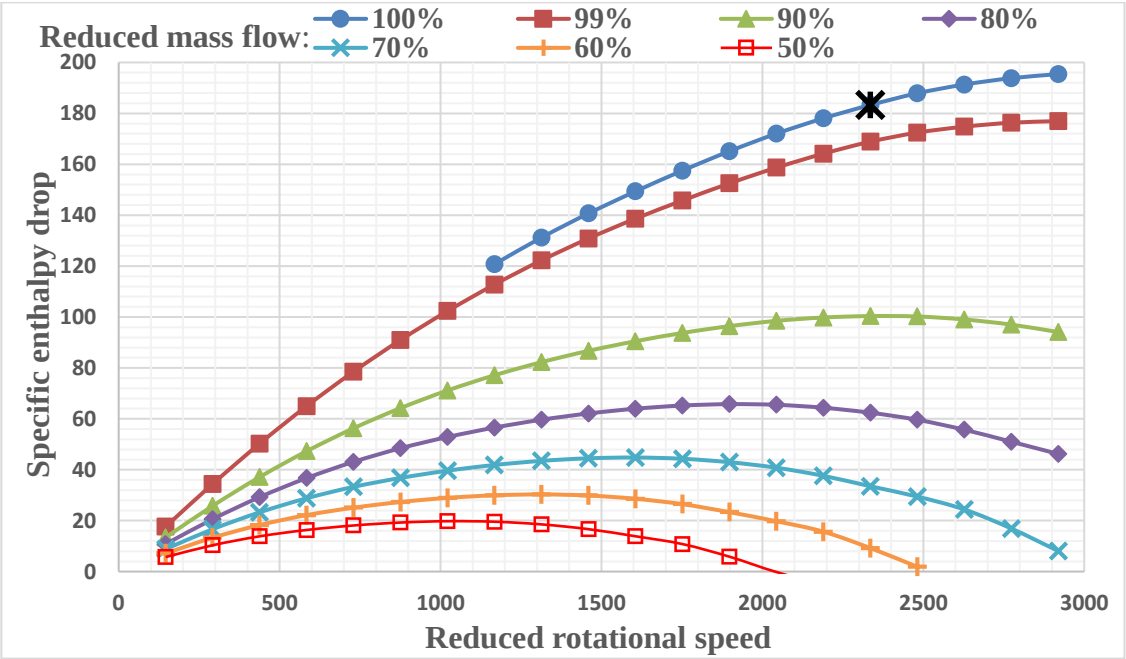

Figure 2.2. Theoretical power map for an axial turbine (3)

Studies on the performance variation of axial turbines have been carried out over time from the desire to predict the behaviour of the turbine at different working regimes. The first and most well-known study in this regard was carried out by Ainley and Mathieson (5), by which a method for calculating turbine performance is proposed. An improvement on this method was made by Dunham. (6) The method is based on empirical approximations, resulting from the experimental research of a significant number of axial turbines, to determine various parameters.

To determine the performances at partial regimes, Petrovici and Reiss (7) proposed a method based on the flow equations and the finite element method. In their paper, the two authors propose the numerical calculation of stage losses by means of loss coefficients such as: profile loss, secondary losses, tip clearance losses and flow mixing at trailing edge for partial regimes. The numerical models for these losses are based on existing studies in the specialized literature and the coefficients are calculated using the parameters of the partial regime.

Since the performance of the turbine decreases when moving away from the nominal regime, the need to adapt the turbine to the input parameters was identified, i.e. an active control of the flow through the vanes. A solution that is successfully used in the case of axial compressors is the use of variable geometry for the fixed section, the stator. The patent for this invention, filed in 1966, belongs to General Electric employees Bell Clarence Edgar Le and Taub Alvin (8). Even though this solution has been proposed for more than 5 decades, it could not be implemented in the case of modern engines due to the extreme temperatures at the turbine inlet, the use of adjustable mechanisms being impossible without affecting the reliability of the engine.

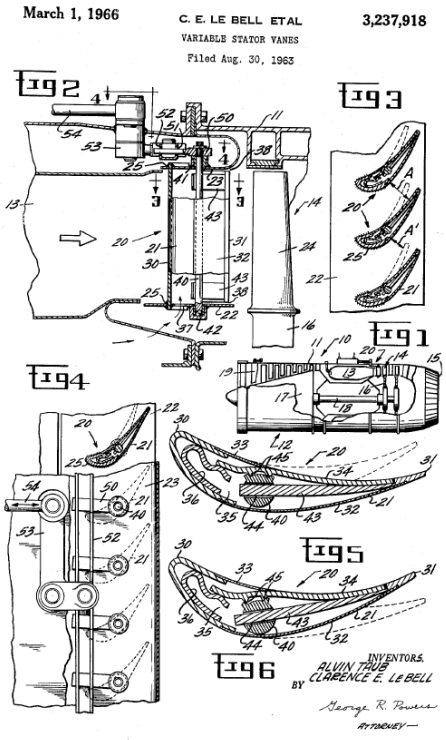

Figure 2.3. Variable vane geometry 1966 (8)

Other methods of active turbine performance control have been proposed by various authors. A performance improvement method based on fluid injection in the boundary layer on

the suction side of the vanes was proposed with as a source of inspiration the active control used in the case of aircraft wings to increase lift and decrease drag. The system uses the injection of a jet of fluid to accelerate the flow on the extrados of the wings thus delaying the occurrence of separations. Studies have shown that a 30% increase in wing efficiency is possible when the injection system is supplemented by a downstream suction process. (9), (10), (11), (12), (13), (14) and (15).

Studies on fluid injection into turbine airfoils were carried out with the aim of reducing pressure losses. In his paper, McQuilling (16) showed that the fluid separation zone on the suction side of a turbine blade can be completely eliminated by using an injection system. By the same study it was shown that the flow of fluid used for injection can be significantly reduced if a pulsating system is used, but its efficiency is strongly influenced by the frequency of the jets. Numerous studies, including (17), (18) and (19), have shown that by using this method fluid separations from the suction side of the profiles can be controlled making the use of high and very high load profiles possible for various applications.

A different approach but with the same goal, that of reducing the losses caused by the appearance of detachments on the extrados of the vanes, was undertaken by Rohr and Yang (20). The authors performed a numerical study in which they used an injection system in the trailing edge area on the vane for a turbine operating at partial regimes. By injecting the fluid into the working channel, a reduction of the section is obtained, resulting in lower pressure gradients, thus reducing the area of detachments on the extrados of the profiles. Similar studies have been undertaken by Postl (21), Galbraith (22), Gross (23), Balzer (24), Saavedra (25)**,** (26), Nowak (27)**,** Wang (28)**,** Padilla (29)**,** Martinez (30)**,** Bernardini (31) etc.

The effects of fluid injection into fixed turbine channels have been intensively investigated in studies of blade cooling methods through film cooling. Thus, numerous studies, including (32), (33), (34), (35), (36), (37) and (38), have investigated the effect of injection direction and flow rate, diameters, distribution and of the number of holes etc. The purpose of injection in the case of cooling is to form a film of fluid that protects the blade material from extreme temperatures and to reduce the impact of the injected fluid on the flow through the channels.

Conclusion

Axial turbines have experienced a continuous process of evolution determined by the evolution of gas turbine engines as a result of the need to improve performance and decrease fuel consumption. Modern turbines today operate at extreme temperatures and pressures while achieving high performance and increased reliability. If the performances of these systems at the nominal regime, the regime at which they are designed, are satisfactory, when moving away from these regimes, that is, when operating at partial loads, the performances of the turbines decrease strongly. A method to adapt the flow regime and turbine performances to these partial regimes has not been successfully identified up to the present moment, the proposed solutions being unable to be implemented due to mechanical considerations or focusing only on the reduction of

some losses. Thus, this work aims to identify a method to improve the performance of these systems depending on the operating regime.

CHAPTER 3 - MATHEMATICAL MODEL FOR DETERMINING THE PERFORMANCE OF AXIAL TURBINES

Fundamental principles of expansion in turbine channels

The fundamental analysis of mechanical work extraction in turbine stages is based on Euler's equation applied to turbomachines, which relates the variation of speeds to the mechanical work produced. The flow through the turbine profiles generally has 3 components, the axial component C, the tangential component C_u, and the radial component C_r.. The axial and radial components of the speeds do not contribute to the energy transfer in the turbine, they are responsible for the gas flow. Figura 3.1 shows the velocity triangles for a plane section through a single-stage axial turbine.

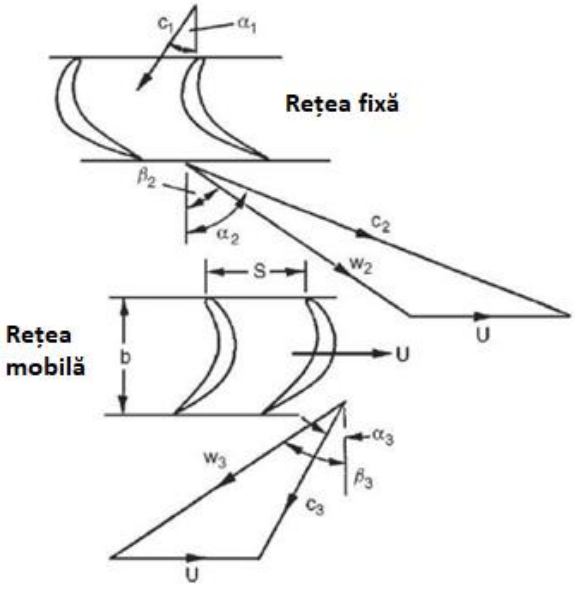

Figure 3.1. Velocity distribution in an axial turbine stage (39)

Combustion gases with a high potential energy (due to the high pressure and temperature) but with low kinetic energy (the speed at the exit from the combustion chamber is low) are accelerated in the fixed profiles, the stator having the role of transforming the potential energy into kinetic energy.

Energy extraction is done by the mobile blades. Thus, the kinetic energy is transformed into mechanical energy in the rotor profiles. The extraction of mechanical work can be done in two ways: by changing the direction of fluid flow, such a turbine is called an action turbine, or by accelerating the gases by forming a converging channel, the turbine being in this case a reaction type. In general, both methods of energy conversion are used, thus the mobile blades achieves both the change of flow direction and the acceleration of the fluid.

Figure 3.2 shows the evolution of the working fluid through the turbine stage, evolution described in h-s coordinates, enthalpy – entropy. The evolution in the fixed profiles (1-2) and in the mobile blades (2-3) is presented. The isentropic evolution corresponding to them (1-2s) and (2-3s) is also presented. The diagram graphically describes the evolution of gases, thus at the entrance to the turbine the kinetic energy is low, being $\frac{1}{2}C_1^2$. Acceleration in the fixed profiles causes the kinetic energy to increase to $\frac{1}{2}C_2^2$. At the entrance to the rotor the relative kinetic energy is low, as can be seen from the diagram, $\frac{1}{2}W_2^2$, the rotor further accelerating the fluid to obtain at the exit from the mobile network a high relative kinetic energy $\frac{1}{2}W_3^2$.

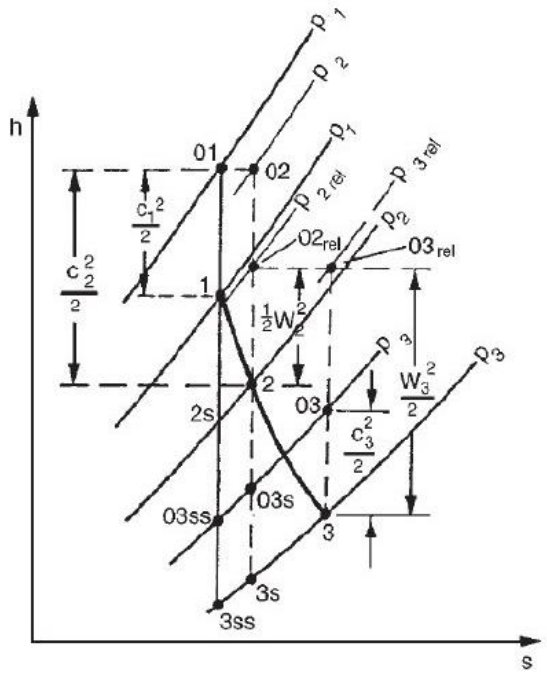

Figure 3.2. Enthalpy - entropy working fluid in a turbine stage (39)

Also from this diagram it can be deduced that the mechanical work produced during the evolution through the turbine stage is equal to the variation of the total enthalpy.

$$W_x = h_{01} - h_{03} \tag{3. 1}$$

, with: W_x – mechanical work;

h_{01} – total enthalpy at turbine inlet;

h_{03} - total enthalpy at turbine outlet;

Assuming a constant vane speed and a constant radius along the moving blades, it follows:

$$W_x = \frac{1}{2}[(W_3^2 - W_2^2) + (C_2^2 - C_3^2)] \tag{3. 2}$$

The efficiency of a turbine stage is defined as the ratio of useful mechanical work (produced) to available mechanical work (equivalent to isentropic process).

$$\eta_{tt} = \frac{h_{01} - h_{03}}{h_{01} - h_{03ss}} = \frac{T_{01} - T_{03}}{T_{01}\left[1 - \left(\frac{P_{03}}{P_{01}}\right)^{(k-1)/k}\right]} \quad (3.\ 3)$$

, where: η_{tt} represents the isentropic efficiency corresponding to the expansion process between the total pressures at the inlet and outlet of the turbine p_{01}, respectively p_{03}.

$$\eta_{ts} = \frac{h_{01} - h_{03}}{h_{01} - h_{3ss}} = \frac{T_{01} - T_{03}}{T_{01}\left[1 - \left(\frac{P_3}{P_{01}}\right)^{(k-1)/k}\right]} \quad (3.\ 4)$$

Flow characteristic at partial loads

In optimal operating conditions, at the nominal regime, the speed triangles are formed in such a way that the relative speed vector W_2 is aligned (or achieves a low angle of incidence) with the leading edge of the rotor. Similarly, the absolute velocity vector at the exit from the rotor is aligned with the fixed profiles corresponding to the next stage or close to the axial direction to avoid the losses introduced by the overrotation of the fluid in the effusor or the elements downstream of the stage. In the case of partial regimes, due to the variation of the input parameters (fluid flow, pressure and temperature), resulting in a variation of the flow velocities, and of the change in the rotation speed of the rotor blades, the velocity triangles that are formed differ from those realized at the nominal regime and the alignment of the flow to the turbine profiles is no longer achieved. In this way, different incidence angles appear than those predicted, thus leading to the introduction of additional losses.

An important role in the decrease of efficiency is represented by the distribution of velocity triangles. Figure 3.3 shows the variation of the velocity triangle with the change of rotation speed.

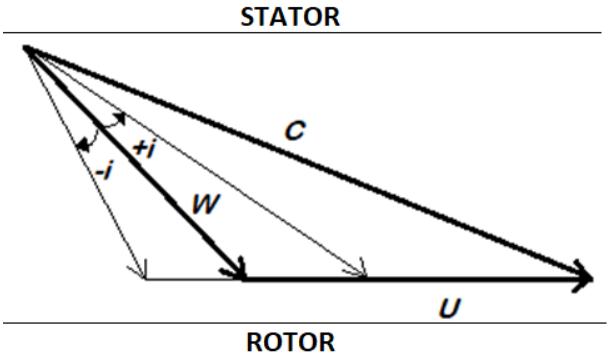

Figure 3.3. Incidence variation as a result of rotational speed variation

The absolute velocity vector, C, is determined by the stator exit angle and the turbine inlet parameters, so it is not affected by the change in rotational speed. The relative velocity vector, W, will thus depend only on the change in speed, which will lead to the change in incidence at the entrance to the mobile network. An increase in speed causes a decrease in incidence, which can

even be negative. Similarly, the decrease in rotation speed, by decreasing the operating regime, causes an increase in incidence.

Figure 3.4 shows the variation of the angle of incidence at the entrance to the rotor blades as a result of flow velocity variation through the channels. Increasing the degree of expansion and fluid flow through the stage results in an increase in absolute velocity. It can be seen from the previous figure that the direction of the absolute velocity vector at the stator exit, C, does not change because this direction is set by the stator geometry. The change in incidence is determined in this case by the increase in absolute velocity resulting, by composing the vectors, in a change in incidence. Increasing speeds causes a positive incidence while decreasing it causes a negative incidence.

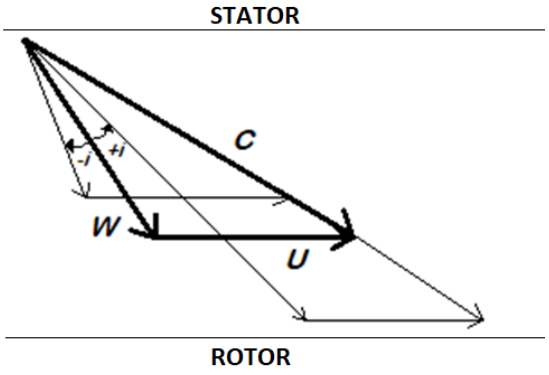

Figure 3.4. Incidence variation as a result of flow velocity variation

A method to determine the losses introduced by changing the incidence at partial regimes was introduced by Mukhtarov and Krichakin (40). They proposed an empirical method for determining profile losses and losses due to secondary flows. This method can be applied for subsonic and transonic airfoils. Thus, the profile losses at any incidence were defined as in the relation (3.5):

$$(1-\Phi^2)_p = (1-\Phi^2)_{p,des} + \Delta(1-\Phi^2)_p \tag{3.5}$$

,with: $(1-\Phi^2)_{p,des}$ – profile losses at the flow angle provided in the design;

$$\Delta(1-\Phi^2)_p = \frac{A}{\left(\frac{D_{LE}}{s}\right)^{0.67}}\left[\left(\frac{cos\alpha_{b2}}{cos\alpha_1}\right)^2\left(\frac{1+\frac{k-1}{2}M_1^2}{1+\frac{k-1}{2}M_2^2}\right)^{\frac{k-1}{k+1}} - \left(\frac{cos\alpha_{b2}}{cos\alpha_{1,des}}\right)^2\left(\frac{1+\frac{k-1}{2}M_{1,des}^2}{1+\frac{k-1}{2}M_2^2}\right)^{\frac{k-1}{k+1}}\right] + \frac{B}{\left(\frac{D_{LE}}{s}\right)^{0.67}}\left(\frac{cos\alpha_{b2}}{cos\alpha_1}\right)^2\left(\frac{1+\frac{k-1}{2}M_1^2}{1+\frac{k-1}{2}M_2^2}\right)^{\frac{k-1}{k+1}} sin^2(\alpha_1-\alpha_{1,des}) \tag{3.6}$$

, for: $\alpha_1 > \alpha_{1,des}$, $A = 0.024$ and $B = 0.144$ and for $\alpha_1 < \alpha_{1,des}$, $A = 0.0007$ and $B = 0.206$

The following notations were made in formula (3.6):

- D_{LE} – leading edge diameter;
- $\alpha_{1,des}$ – nominal regime velocity angle;

-α_{b2} - geometry exit angle;

Losses due to secondary flows for any incidence are calculated as follows:

$$(1-\Phi^2)_s = (1-\Phi^2)_{s,des} + \Delta(1-\Phi^2)_s \quad (3.\ 7)$$

,with: $(1-\Phi^2)_{s,des}$ - losses due to secondary flows at the flow angle provided in the design;

$$\Delta(1-\Phi^2)_s = (1-\Phi^2)_{s,des}(5.6\chi + 76\chi^2 + 400\chi^3) \quad (3.\ 8)$$

,with:

$$\chi = \frac{\alpha_1 - \alpha_{1,des}}{180 - (\alpha_1 + \alpha_{b2})}\left(\frac{cos\alpha_{b2}}{cos\alpha_{1,des}}\right)^2 \quad (3.\ 9)$$

, the relation being valid for $-0.15 \leq \chi < 0.15$.

Another method to approximate the losses introduced by the change in incidence was proposed by Ainley and Mathieson (5). This method is based on the estimation of the positive incidence which has been correlated with the pitch/chord ratio and the flow angles at the outlet and inlet of the profiles. The incidence is calculated according to the following relationship:

$$i_s = i_s(s/c = 0.75) + \Delta i_s \quad (3.\ 10)$$

,with i_s - the critical angle of incidence, defined as that angle at which the profile losses are double the case of zero incidence;

$i_s(s/c = 0.75)$ - critical angle of incidence for to an incidence with $s/c = 0.75$;

Δi_s - the induced angle of the gas flow, is calculated using the graph in Figure 3.5.

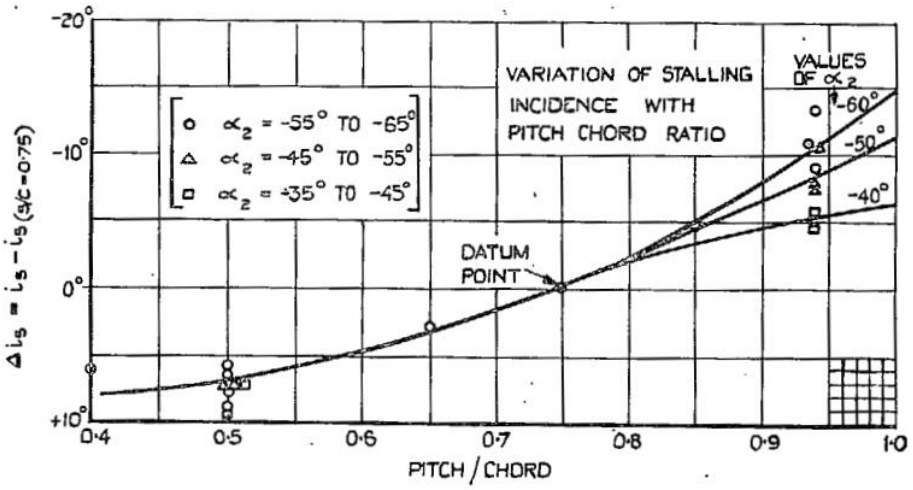

Figura 3.5. Incidence variation for real profiles and the incidence for profiles with s/c=0.75 (5)

The exit flow angle is determined using the graph in Figure 3.6 and this value is then used to determine the critical incidence for a grid with s/c=0.75 using the graph in Figure 3.7.

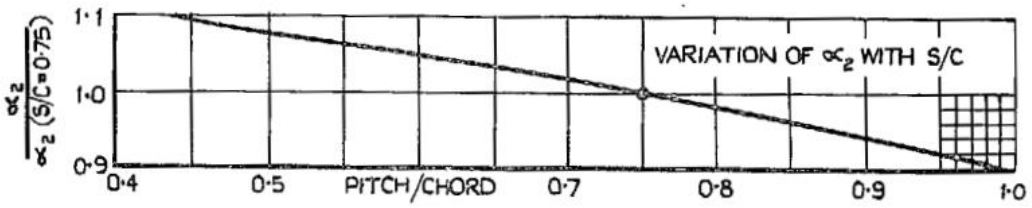

Figure 3.6. Exist flow angle variation as a function of s/c (5)

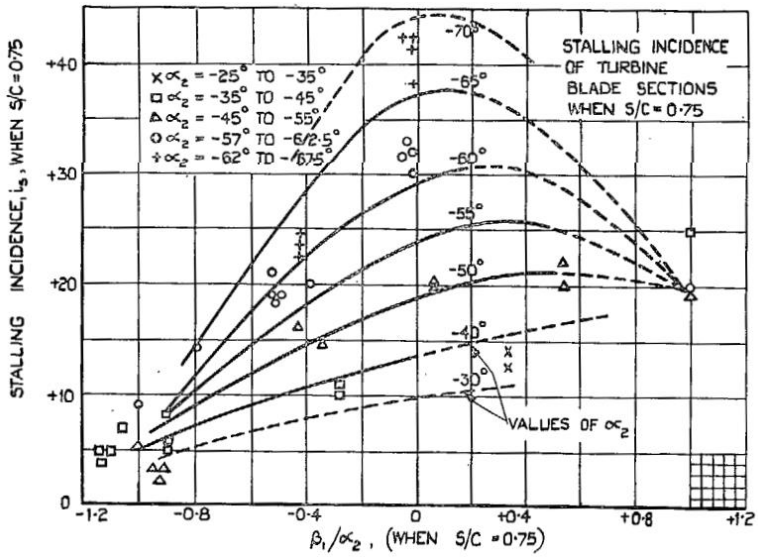

Figure 3.7. Critical incidence variation for blades with s/c=0.75 (5)

Determination of the profile losses is carried out by determining the ratio between them and the profile losses at incidence 0 considering $Re = 2\ x\ 10^5$ and $M < 0.5$. The variation of this ratio with relative incidence, the i/i_s ratio, is shown in Figure 3.8.

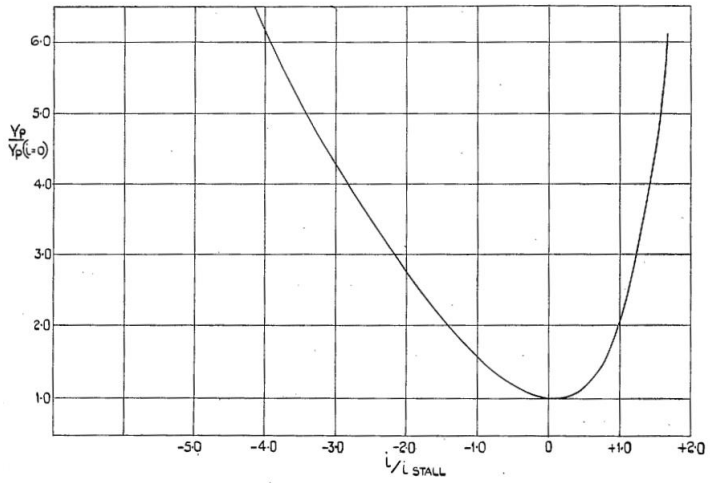

Figura 3.8. Variația pierderilor de profil cu incidența (5)

Conclusion

The operation of the turbine at partial working regimes causes a change in the velocity triangles over the entire height of the blades in the 3 sections of interest. This change is caused by the change in the gas-dynamic parameters at the turbine inlet, but also by the change in the rotation speed as a result of the change in the load consumed by the compressor or another consumer. Since the geometries of the profiles are fixed (non-adjustable), the power developed by the turbine is determined, according to the Euler equation, by the resulting velocity triangles.

It is thus possible to identify the need to control the velocity triangles at partial regimes in order to increase the power developed by the turbine at the respective regimes. In this work, a method is proposed to increase the performances at partial regimes by increasing the speed at the exit from the vanes at the regimes for which it is applied. By injecting the fluid, the aim is to reduce the passage section at the exit from the stator to accelerate the working fluid, which causes an increase in the power developed by the rotor according to the Euler equation. A schematic of the proposed injection system is shown in Figure 3.9.

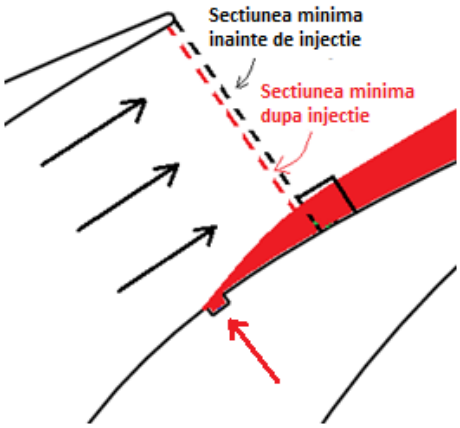

Figure 3.9. Proposed vane injection system

CHAPTER 4 - RESEARCH METHODOLOGY OF THE FLOW CONTROL METHOD IN THE BLADED CHANNELS OF AXIAL TURBINES

A method of controlling the performance of axial turbines, at partial regimes, by using a fluid jet is proposed. The aim is thus to determine the conditions, both gas-dynamic (injection fluid flow, pressure, temperature) and geometric conditions (diameter of the injection hole, their position and number), characteristic of each partial regime with the aim of obtaining an improvement in performance.

In order to determine the optimal configuration of the injection system, the research of the influence of the different parameters on the flow and performance of the turbine is pursued. In this sense, it is necessary to establish a research methodology by defining geometry and a reference case, the parameters of interest and a test matrix. Figure 4.1 presents the theoretical research methodology.

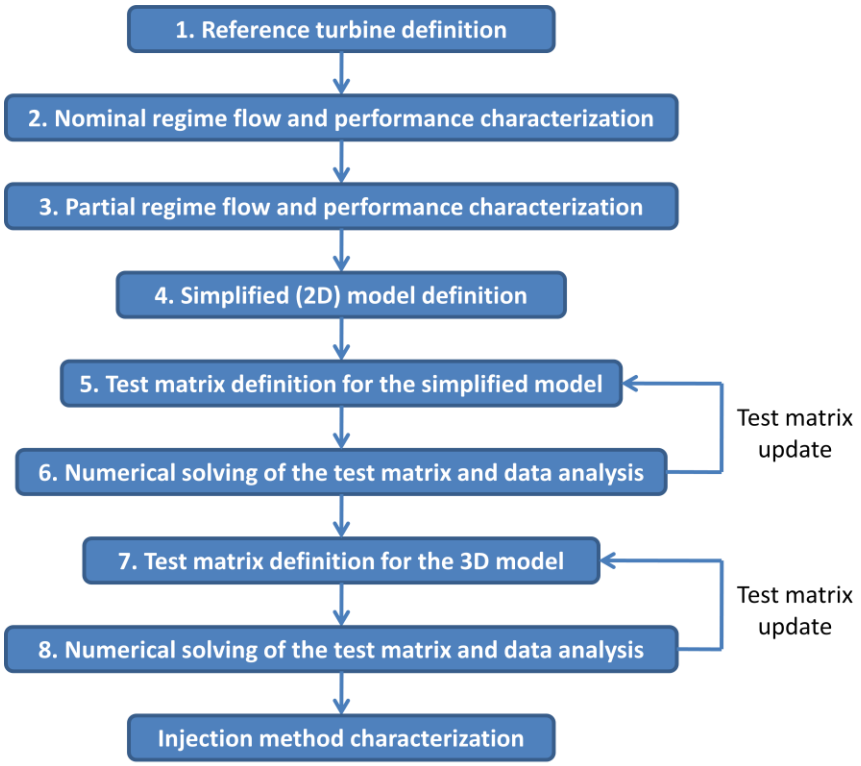

Figure 4.1. Research methodology for injection method characterization (41)

Reference turbine definition

To study the method of controlling the flow through the axial turbine channels, a power turbine whose geometry is known was chosen. The turbine develops, at nominal regime, a power of 1350 KW, the mass flow rate being 8 kg/s. The characteristic parameters of the turbine are presented in Table 4.1.

Table 4.1. – Reference turbine parameters

Nr. crt.	Parameter	Value
1	Turbine type	Action-reaction
2	Vane hub radius [mm]	136.7
3	Vane shroud radius [mm]	190.6
4	Rotor exit hub radius [mm]	123.8
5	Rotor exist shroud radius [mm]	235
6	Tip clearance [mm]	1
7	Number of vanes	44
8	Number of blades	53
9	Mass flow [kg/s]	8
10	Total inlet temperature [K]	977
11	Total inlet pressure [barA]	2.55
12	Rotational speed [rpm]	22000
13	Generated power [KW]	1350

14	Pressure ratio	2.1
15	Isentropic efficiency [%]	87

Turbine channels flow characterisation at nominal regime

Flow characterisation through the channels of the reference turbine was carried out by numerical calculation using commercial software, namely ANSYS CFX. Through this calculation, the performance of the turbine was validated and the characteristics of the flow through the turbine networks were determined. This data (in particular the velocity and flow regime through the fixed networks) will be used for comparison with the results obtained from the injection process. To calculate the nominal regime, the total pressure and temperature at the stage inlet, the rotational speed and the mass flow of the working fluid were imposed. The boundary conditions, as defined for this case, are shown in Table 4.2.

Table 4.2. – Boundary conditions for nominal regime

No.	Type	Location	Observation
1	INLET	Vane inlet	Total pressure = 2.55 barA Total temperature = 977 K
2	OUTLET	Rotor outlet	Mass flow = 8 kg/s
3	WALL	Vane - hub - shroud - blade Rotor - hub - shroud - blade	Adiabatic no slip walls
4	PERIODIC interface	Lateral delimitation of the fluid volume of the vane or the rotor	Rotational perodicy, fluid-fluid interface
5	STAGE interface	Vane exist – Rotor inlet	Fluid-fluid interface

Turbine channels flow characterisation at partial regime

For the calculation of the partial regime, turbine inlet conditions as well as turbine rotational speed for a lower power regime were determined. An operating mode of the approximately 89% gas generator speed was thus chosen, resulting in the turbine operating conditions presented in Table 4.3. Partial regime calculation was carried out using the same assumptions and numerical grids as in the case of the calculation of the nominal regime, the results being presented in Table 4.4.

Table 4.3. – Partial regime inlet parameters

No.	Parameter	Value
1.	Inlet total pressure [barA]	2.34
2.	Inlet total temperature [K]	868

3.	Mass flow [kg/s]	7
4.	Rotational speed [rpm]	20000

Table 4.4. – Partial regime main results

No.	Parameter	Value
1.	Generated power [KW]	466.6
2.	Isentropic efficiency [%]	87.2
3.	Pressure ratio	1.37
4.	Outlet total temperature [K]	801
5.	Vane maximum speed [m/s]	402
6.	Vane exit flow angle [grade]	65.3

Similar to the nominal regime, the flow field does not present areas with significant detachments; however, compared to the previous case, the incidence angle of the flow in the rotor differs due to the change of the velocity triangle. Another consequence of the decrease in the working regime is the reduction of the flow regime in the turbine vanes. It can be noted, analyzing Figure 4.2, a significant decrease in Mach number in the stator, compared to the nominal regime.

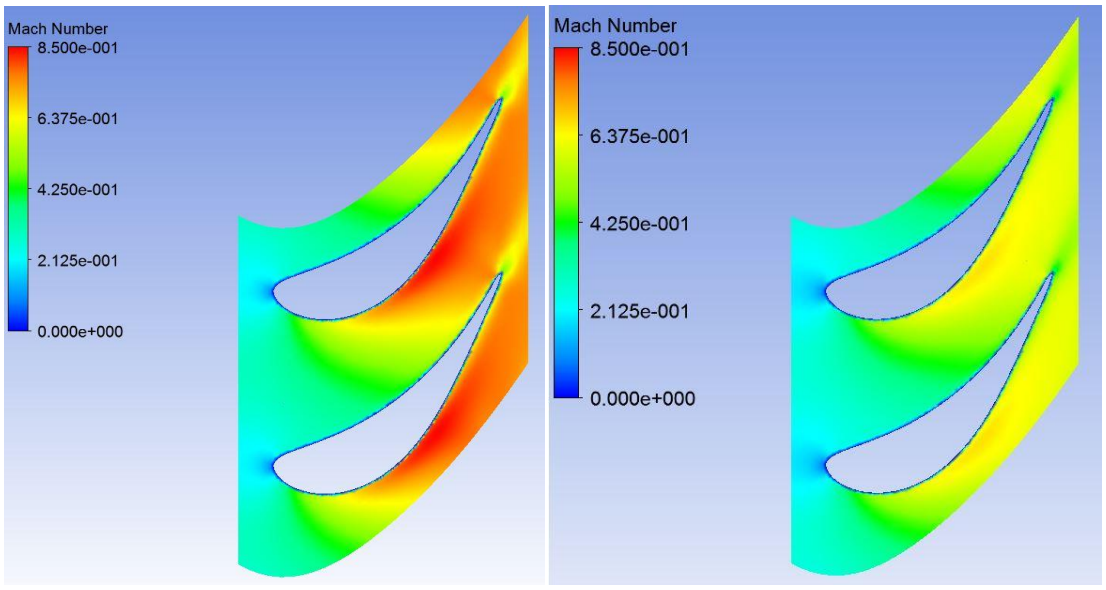

a. b.

Figure 4.2. Mach number at mean radius for: a. nominal regime, b. partial regime

The possibility of improving the performance for the reference turbine at partial regime by accelerating the working fluid in the vanes and changing the velocity triangle at the rotor inlet is thus identified.

Definition of 2D simplified model

In order to define an optimal configuration of the injection system, it is necessary to research the influence of different geometric and gas-dynamic parameters on the performance of the reference turbine at partial regime. Thus, it is necessary, in a first phase, to reduce the calculation volume, this being possible by using a simplified 2D model.

Next, the flow through the fixed networks in the plane will be analyzed, the stator profile being that of the mean radius. Figure 4.3 show the geometry of the 2D model. The solution of the numerical simulation of a number of 4 vanes was chosen to reduce possible errors due to the use of periodic conditions on the two lateral areas.

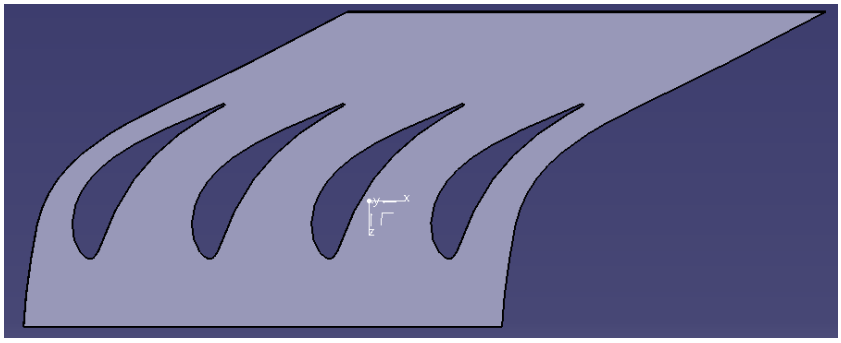

Figure 4.3. 2D model geometry (41)

For the simplified model, the flow field was determined both at the nominal regime and at the partial regime. The ANSYS CFX software was used to calculate the flow, and the ANSYS Meshing software was used to create the numerical grid. Also, the boundary conditions are similar to the previously described cases.

Since the simplified 2D model does not incorporate the rotor profile, the calculation being made only for the vanes, the parameters of interest in the case of the 2D model will be the speed and the exit angle from the stator and the total pressure loss in the vanes. Thus, through fluid injection, the aim is to increase the exit velocity from the stator (value averaged over the exit area), change the velocity triangle, but also maintain pressure losses on the stator within certain limits.

Test matrix definition

In order to define a test matrix, based on which the characterization and optimization of the injection system will be carried out, it is necessary to identify the parameters of interest for this injection system. Next, the two categories of parameters of interest are presented:

- Gas-dynamic parameters:

- flow regime: only subsonic flow regimes will be considered to eliminate possible losses due to shock waves.

-injection fluid total temperature: the temperature range [400:900] °C will be considered.

- injection fluid total pressure: the maximum pressure will be approx. 15.

- injection mass flow: a fluid mass flow of maximum 5% is considered. This value was chosen by analogy with the flow rate taken for cooling the turbine.
- injection fluid velocity: it will be determined by the previously described parameters and the diameter of the injection holes.

- Geometrical parameters:

- axial distance (z_a): will be quantified by using a ratio of the minimum distance between the stator vanes to the axial distance from the area of the minimum section to the center of the injection port. The axial distance is calculated according to equation (4. 1), the terms being defined in Figure 4.4.

$$z_a = \frac{a}{b} \tag{4. 1}$$

, with: a – the distance from the point of minimum section to the center of the injection hole;
b – minim section of the vanes.

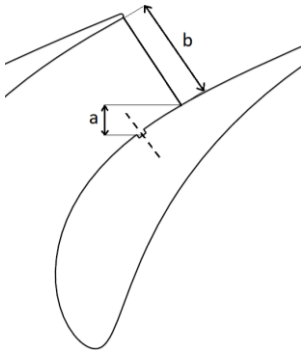

Figure 4.4. Positioning of injection orifice (41)

- injection angle: it represents the angle formed by the flow direction of the injection fluid relative to the flow direction of the working fluid in the area of the injection hole. Injection angle values between 30 and 90 degrees will be tested.
- diameter of the orifices: will be determined based on gas dynamic considerations, reaching an almost transonic regime with an injection flow rate of maximum 5% of the flow of the working fluid, a maximum pressure of 15 bar and a maximum temperature of 900 °C.
- number of orifices: the number of injection holes will be determined along the way based on the intermediate results.

CHAPTER 5 - NUMERICAL STUDY REGARDING THE METHOD OF INCREASING PERFORMANCE THROUGH FLUID INJECTION - 2D MODEL

Next, the determination of the influence of previously established parameters on the flow through the channels of the simplified model is considered. In a first stage, the following parameters were selected: injection fluid flow, the angle at which the fluid is injected (relative to the direction of flow of the working fluid), axial distance of the injection hole (relative to the critical area of the profiles), the diameter of the injection orifice, and the temperature of the injection fluid.

Numerical cases definition – fluid

Through the variation of the previously presented parameters, a number of 101 numerical cases resulted. Due to a large number of cases, the parametric mode available in the ANSYS CFX commercial software was used with which the numerical study was carried out.

The numerical cases and boundary conditions for the numerical studies in which the injection holes were introduced were set in such a way that the comparison with the previously determined case without injection could be made. Thus, the numerical grid and the boundary conditions were maintained, and the boundary conditions for the injection holes were added.

Injection angle influence

The influence of the injection angle on the evolution of the flow through the vanes was determined by carrying out several numerical cases in which only the direction in which the fluid is injected was changed compared to the direction of the flow of the working fluid in the injection zone.

The increase in the injection angle determines, in a first phase, the distance of the injected fluid from the suction side of the vane, fluid which then, through the interaction with the working fluid, changes its flow direction in the direction of the working fluid flow. This is due to both the interaction of the two fluids and the pressure gradients. Following the injection, a low-pressure area is formed downstream of the injection orifice, which influences the flow of the fluid after the injection (Figure 5.1). Through the injection into turbine vanes and the formation of the previously described phenomenon, a reduction of the section through which the working fluid passes is achieved, and if this section is in the area of the minimum section, the acceleration of the fluid takes place compared to the case without injection.

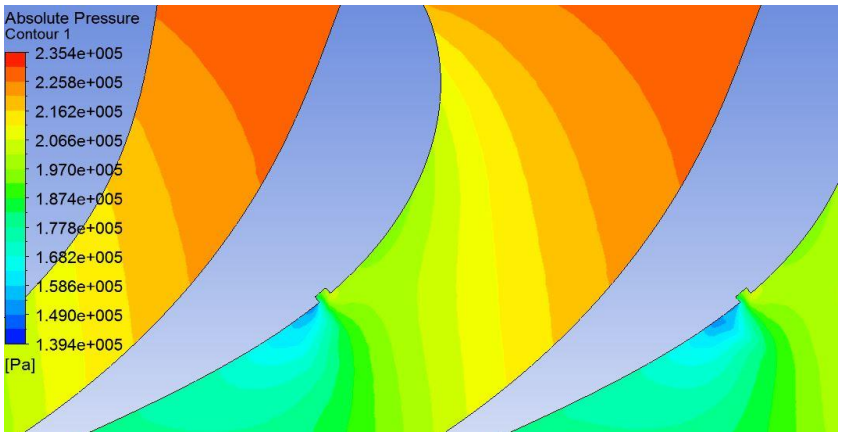

Figure 5.1. Low pressure zone formed downstream of injection orifices (41)

Figure 5.2 show the evolution of the average speed at the exit from the fixed network for different values of the injection angle and for 3 values of the injection flow rate. An important increase in speed can be observed when changing this parameter, the evolution being similar to changing the injection speed (resulting in this case as a result of increasing the flow of fluid through the same orifice).

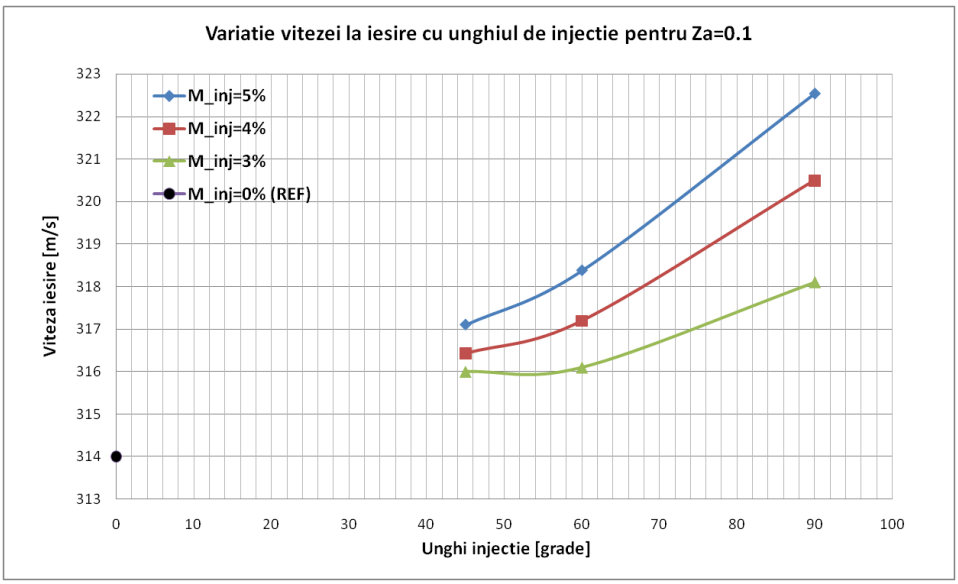

Figure 5.2. Mean vane exist velocity variation with the injection angle

Injection mass flow influence

For a constant injection orifice diameter and constant gas-dynamic parameters of the injection fluid, increasing the injection flow rate increases the rate at which the fluid is injected into the working channel of the vanes. Increasing the injection speed causes an increase in the low pressure area which leads to a decrease in the minimum section and thus to an increase in the velocity through the vanes. The influence of increasing the injection flow rate can be determined from Figure 5.3 by analyzing the influence on the speed at the vanes.

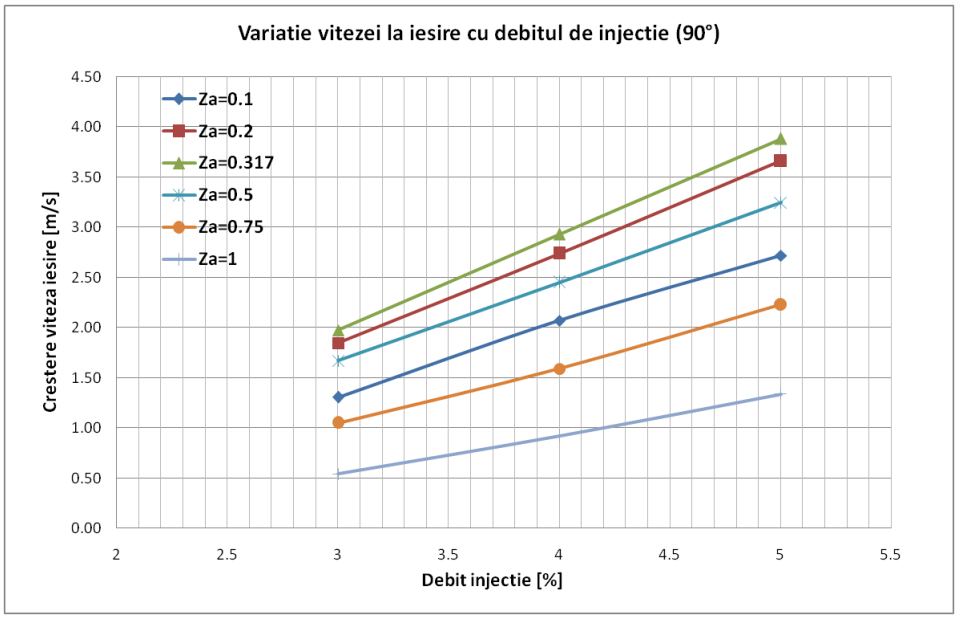

Figure 5.3. Mean vane exist velocity variation with the injection mass flow

From the analysis of the influence of the injection mass flow on the maximum speed through the vanes, it follows that an increase of more than 12% is possible with an injection mass flow of 5%. From the analysis of the evolution of pressure losses, it follows, as expected, that at a higher value of the injected mass flow, and implicitly a higher value of the speed of the injected fluid, an increase in pressure losses results.

Axial distance influence

The axial placement of the injection sections in the vanes plays an important role in influencing the performance of the injection system. The formation of the low pressure area that causes the minimum section to decrease is more effective if it occurs near this minimum section. If the top of this "bubble" coincides with the minimum section, the efficiency of the injection system is high because in this way the best constraint of the section is obtained using the available fluid.

Figure 5.4 shows the variation of the average speed at the exit from the vanes with the axial distance at which the injection is made. The presented case assumes fluid injection at 90° to the working fluid flow direction and a flow rate of 5%. One can identify the presence of a position where the curve reaches a maximum, Za≈0.27.

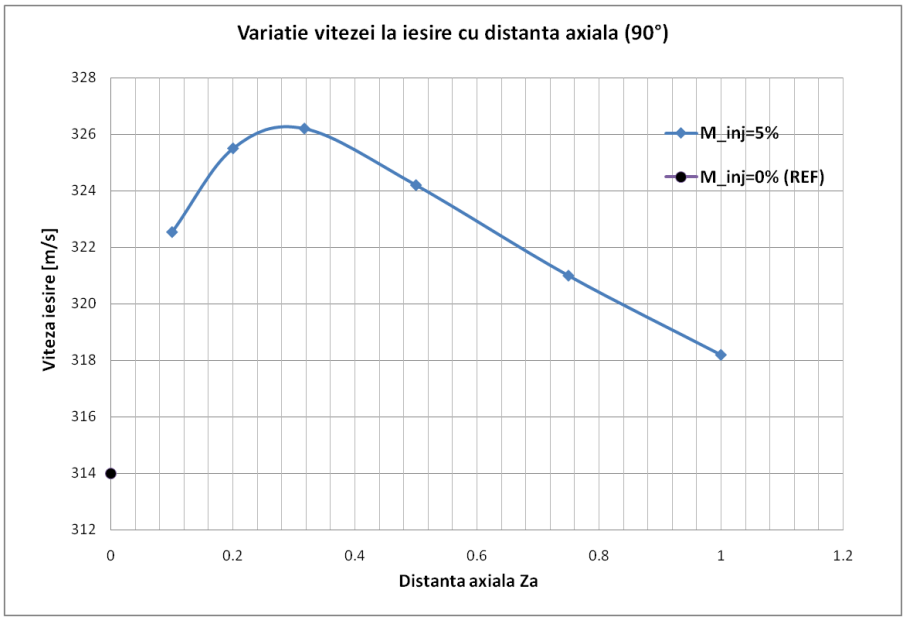

Figure 5.4. Mean vane exist velocity variation with the axial distance (41)

In the case of pressure losses, their variation with axial distance is low, being higher in the case of injection in the area of the minimum section, but by distancing from this area, and the streamlining effect, causes a decrease in losses.

Injection orifice diameter influence

The diameter of the injection section directly influences the injection velocity, if the injection mass flow and fluid input parameters (pressure, temperature) remain constant. As previously mentioned, the speed has an important influence on the flow evolution in the vanes. It is aimed, by reducing the injection hole, to obtain similar effects but with a lower injection mass flow. Injection orifices of 0.8, 0.6, 0.5 and 0.4 mm were taken into account, due to considerations related to the possibility of their manufacture. It can be noted the decrease of the injection effect on the speed in the vane when the injection diameter increases. This evolution can be explained by the decrease in the injection speed and the decrease in the amplitude of the low pressure zone. From Figure 5.5 an increase in the low pressure area (green area) with decreasing injection diameter can be determined.

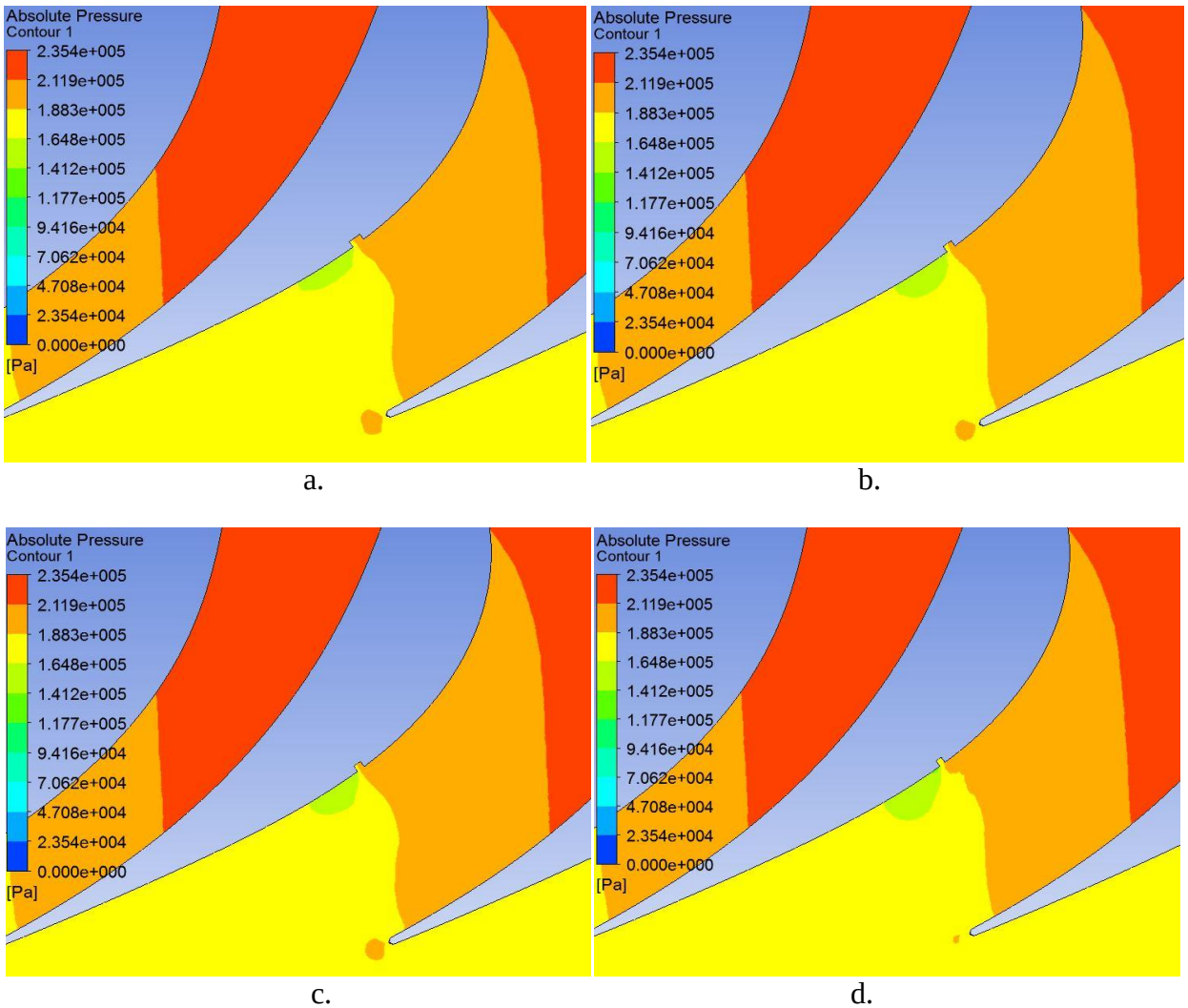

Figure 5.5. Static pressure distribution for an orifice diameter of: 0.8 mm (a.) , 0.6 mm (b.), 0.5 mm (c.) and 0.4 mm (d.) for $\dot{M}_{inj}$=5% and $\alpha_{inj} = 90°$, Za=0.2 (41)

Injection fluid temperature influence

In addition, the influence of the injection fluid temperature was also determined. If in the previously presented cases the total temperature of the injection fluid was 868 K, an analysis was carried out by changing the temperature of the injection fluid in the range [718 K - 1118 K]. By increasing the injection temperature, the injection speed is increased, which leads to an increase in the influence of the injection system on the flow through the vanes. It can be seen from Figure 5.6, which shows the variation of the velocities at the vane exit relative to its value before injection with the temperature of the injection fluid, an almost linear variation of the speed increase with the increase of the injection temperature.

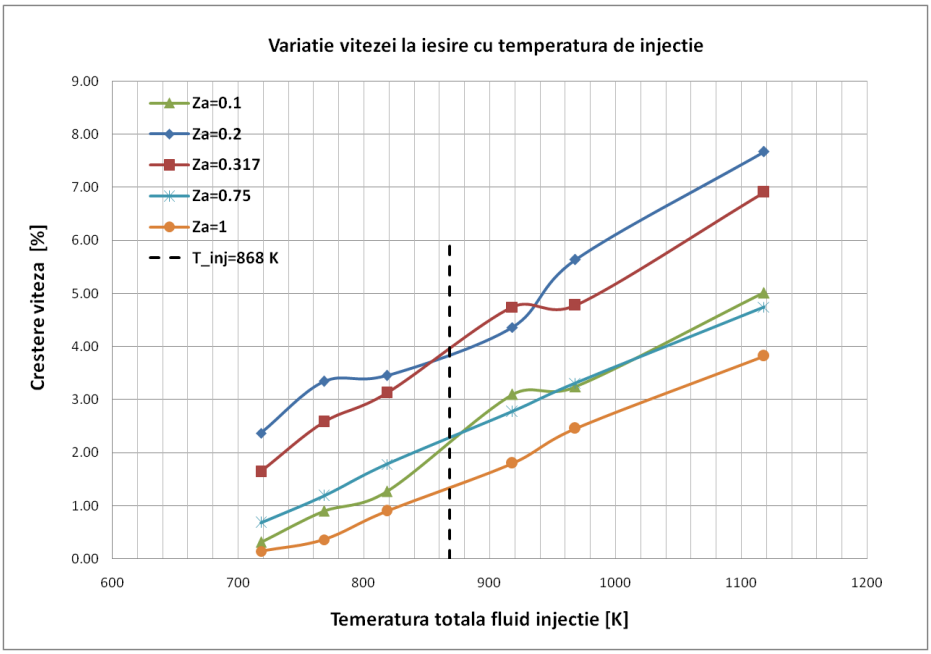

Figure 5.6. Mean vane exist velocity variation with the injection fluid temperature

CHAPTER 6 - NUMERICAL STUDY REGARDING THE METHOD OF INCREASING PERFORMANCE BY FLUID INJECTION - 3D MODEL

Next, the influence of the geometric parameters on the performance of the turbine on the 3D model is considered. As a first step, the following parameters were selected: the diameter of the injection holes, the axial distance of the injection hole (relative to the critical area of the profiles) and the number of injection holes.

Three dimensional model construction

To generate the geometry incorporating the injection system, it was necessary to determine the critical section of the vanes. Thus, the intersection of the critical section with the suction side of the vanes was determined by geometrically measuring (on the 3D model) the minimum distance of the vanes at different radius. For the reference turbine, the minimum section and its position on the suction side was determined in 7 sections and by joining them a

curve was made on the suction side. By translating upstream this curve with different values according to the desired axial distance (Za) on the suction side, the position of the injection sections is obtained. After establishing the positioning curve of the orifices, their diameter and number as well as the distance between the holes were determined. In the studies presented in this paper, injection section equidistant between the hub and shroud were used. The injection system generation process for the 3D model is shown in the flowchart in Figure 6.1.

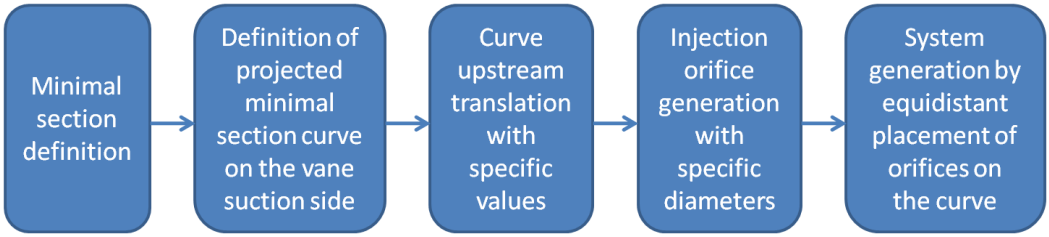

Figure 6.1. Steps for injection model generation (42)

The numerical grid was established by determining its influence on turbine performance. Thus, 4 configurations of the grid were established, increasing the number of elements by 2.5 times and carrying out the numerical analysis of the turbine performances for each configuration. For this unstructured numerical grid, the cells have an overall size of 1 mm, being dense near the walls and near the injection holes.

The turbulence model and boundary conditions for the numerical studies with the injection system were established in such a way that the comparison with the previously determined no-injection case could be made. Thus, the boundary conditions were kept, adding those related to the injection holes. Table 6.1 shows the boundary conditions used.

Table 6.1. – Boundary condition for 3D model

No.	Type	Location	Observation
1.	INLET	Vane inlet	Total pressure = 2.34 barA Total temperature = 868 K
		Injection section inlet	Mass flow = 2.5 % total mass flow Total temperature = 868 K
2.	OUTLET	Rotor outlet	Mass flow =7 kg/s
3.	WALL	Model walls	Adiabatic no slip walls
4.	PERIODIC interface	Lateral delimitation of the fluid volume of the vane or the rotor	Rotational periodicy, fluid-fluid interface

Injection orifice diameter influence

The influence of the diameter of the injection sections was also analyzed in the case of the 2D model, the results showing that the deflection of the working fluid is more pronounced in the case of small values of the diameter of the orifices as a result of the injection speed increase. In this chapter, the influence of the dimensions of the injection sections will be analyzed from the

point of view of their distributions on the radius. For each diameter, a number of sections were determined so that when injecting the same fluid flow, the Mach number through the orifices is approximately the same. For this analysis, only the diameter of the orifices, their number and the axial distance are varied. Thus, it is ensured that the injection speed is approximately the same regardless of the diameter of the sections.

For an injection diameter $Ø_{inj} = 0.5\,mm$, a number of 76 injection sections was established, the performance of the turbine being determined for 4 values of the axial distance, $Za = 0.1,\ 0.2,\ 0.317\ and\ 0.5$. The variation of the axial distance causes a variation of the turbine performances, as demonstrated on the simplified 2D model, with a maximum of the influence around the value Za≅0.27. From the analysis of the results it emerged that the greatest influence on the flow through the vanes is obtained for small values of the diameter of the injection holes.

From Figure 6.2 it follows that the power developed by the turbine decreases with the increase in diameter up to a value of 0.8 mm. Further increasing the diameter of the holes to $Ø_{inj} = 1\,mm$ does not produce major changes. An increase of approximately 33% in turbine power can thus be observed in the case of a small diameter of the holes.

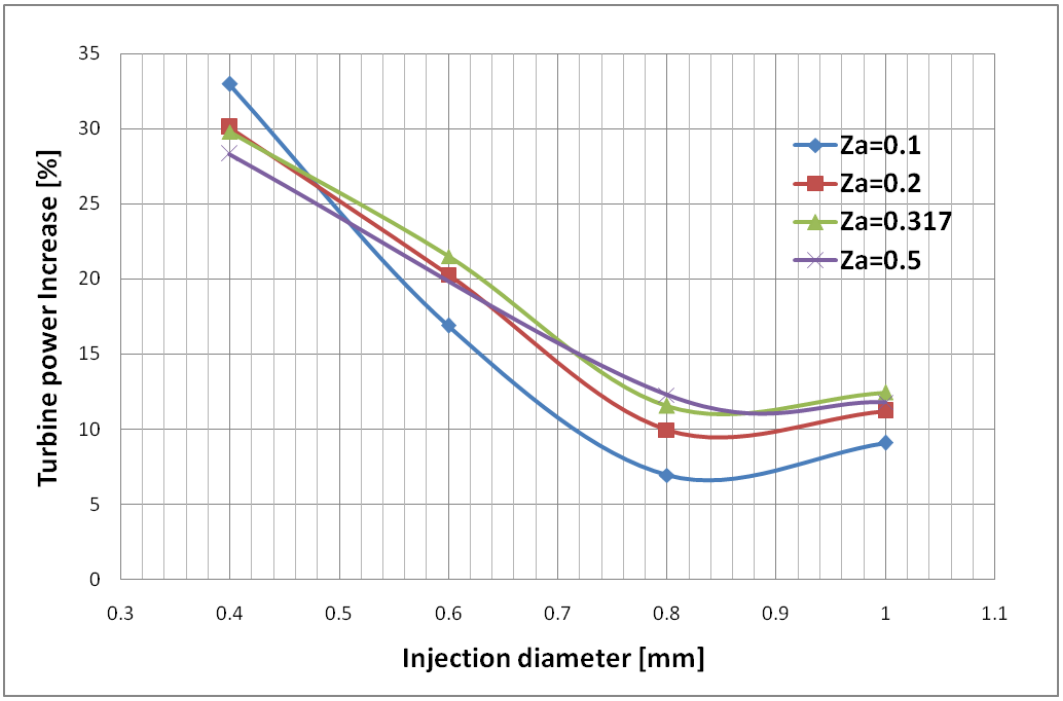

Figure 6.2. Turbine power increase for different values of the injection sections diameter and axial distances (42)

Figure 6.3 shows the comparison of the total pressure through the vanes at mean radius between the case without and with injection. The narrowing of the critical section following injection can be seen from this comparison.

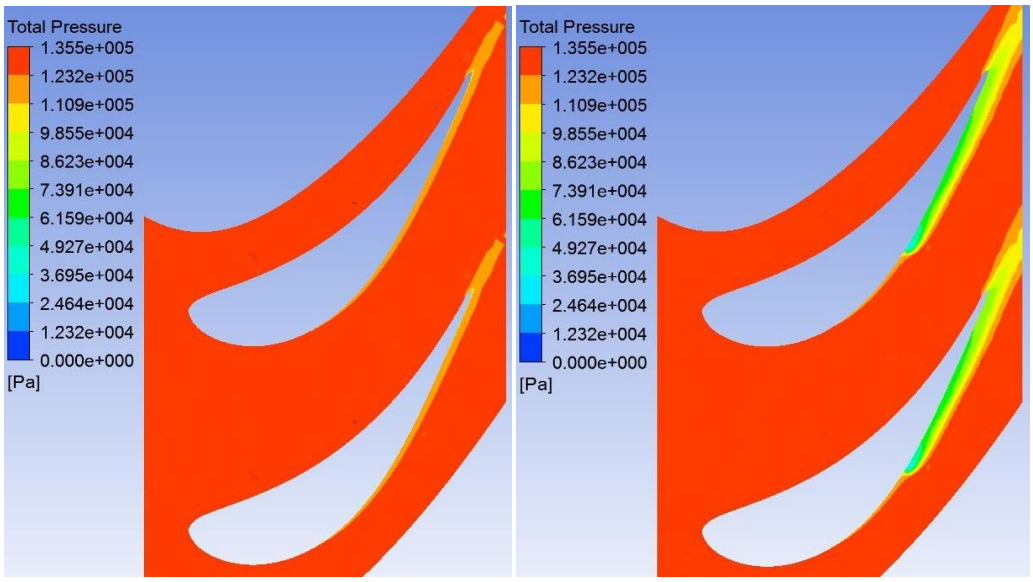

a. b.

Figure 6.3. Mean radius total pressure comparison for: a. no injection and b. with injection (42)

When the diameter of the injection sections increases and implicitly when the number of sections decreases, the distance between them grow, so the working fluid will be diverted only in the area adjacent to the sections, there are areas where the deviation of the working fluid is low. This can be noted in Figure 6.4 which show the total pressure distribution in a section downstream of the injection sections for the 4 orifice sizes studied. It can be seen that for small diameter values (0.5 and 0.6 mm respectively) the working fluid deflection is continuous along the vane radius while for larger diameters (0.8 and 1) the working fluid passes between the injection sections.

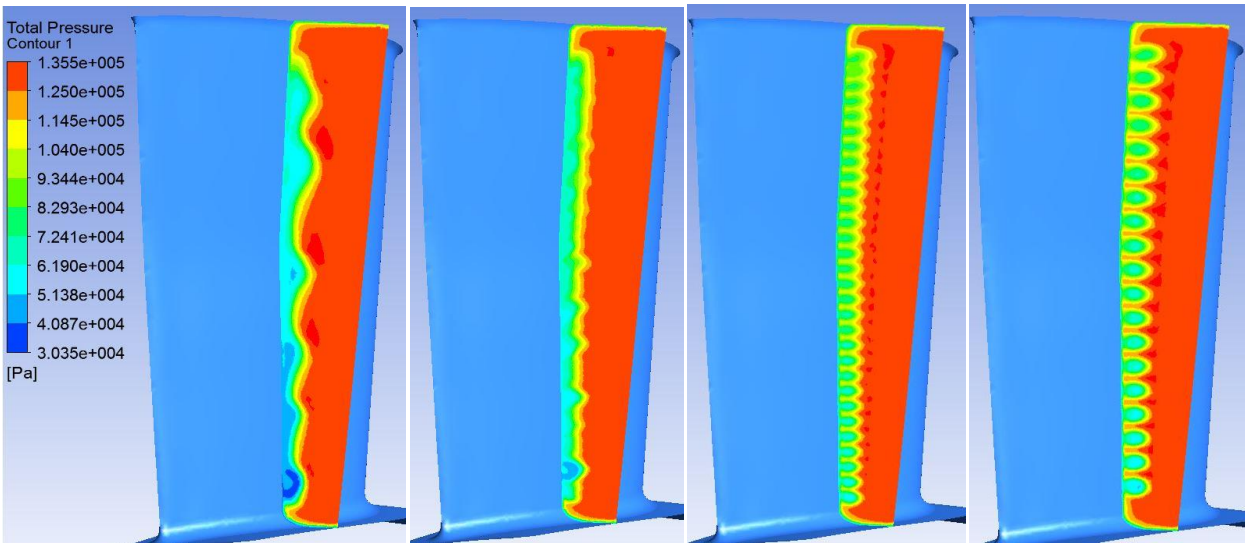

a. b. c. d.

Figure 6.4. Mean radius total pressure comparison in a downstream section for: $\emptyset_{inj} = 0.5\ mm$ (a.), $\emptyset_{inj} = 0.6\ mm$ (b.), $\emptyset_{inj} = 0.8\ mm$ (c.) and $\emptyset_{inj} = 1\ mm$ (d.) (42)

Injection sections number influence

In order to determine the influence of the number of orifices, the performance of the turbine was determined when increasing the number of injection sections while keeping the inlet parameters of the injection fluid as well as the diameter of the orifices constant. For this analysis, the calculations were made for an injection diameter$\emptyset_{inj} = 0.6\,mm$, $Za = 0.2$ and a number of orifices between 53 and 70. The variation of turbine power when increasing the number of orifices is shown in Figure 6.5. Also shown in this graph is the drop in injection speed (Mach number) for the studied points. An approximately linear increase in the power developed by the turbine can be observed, resulting in an increase of approximately 8% between the cases studied (between 53 and 70 holes).

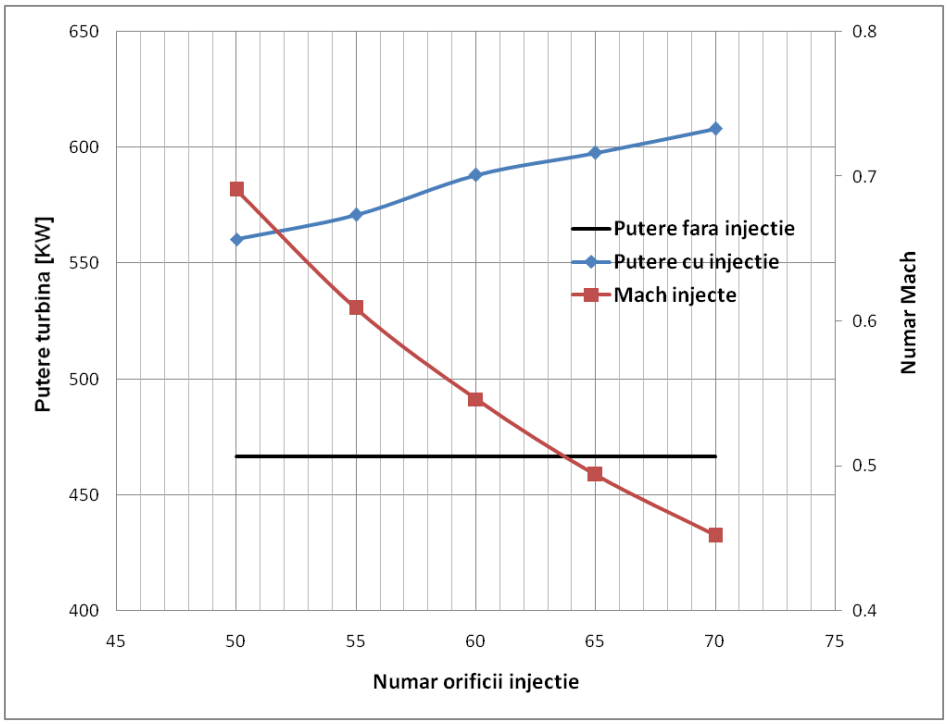

Figure 6.5. Turbine power and injection Mach number variation with the number of orifices

To describe the influence of the number of sections in relation to the dimensions of the turbine, a new parameter is introduced, called coverage degree ($\boldsymbol{\tau}$), defined as the percentage of the height of the working channel covered by orifices in the injection section.

By graphically representing the variation of power resulting from the injection with the variation coverage degree, Figure 6.6., a direct relationship between the two parameters is observed. Thus, when the coverage degree increases, an almost linear increase in the power generated by the turbine is obtained following the injection.

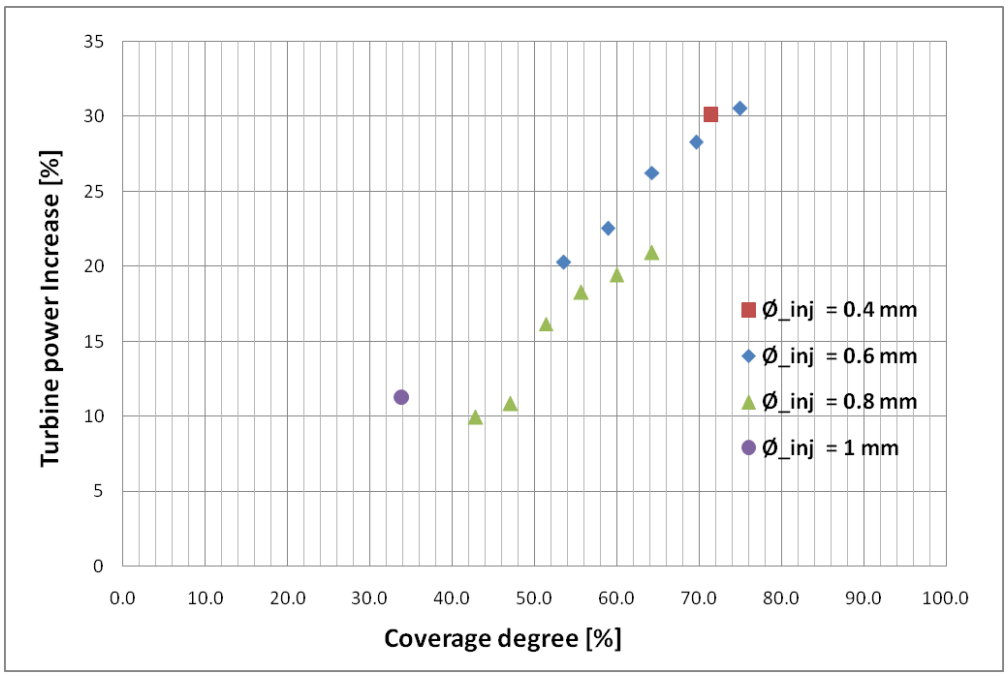

Figure 6.6. Turbine power variation with the covarage dregree (42)

In Figure 6.7, which shows the contour of the total pressure in a plane downstream of the injection section, differences at the increase of the number of orifices and implicitly the degree of coverage can be seen. The compared cases correspond to a diameter$Ø_{inj} = 0.6, Za = 0.2$, 53 and 70 holes respectively. A homogenization of the area adjacent to the injection section can be observed, thus the working fluid does not pass between the injection holes as a result of the reduction of this space.

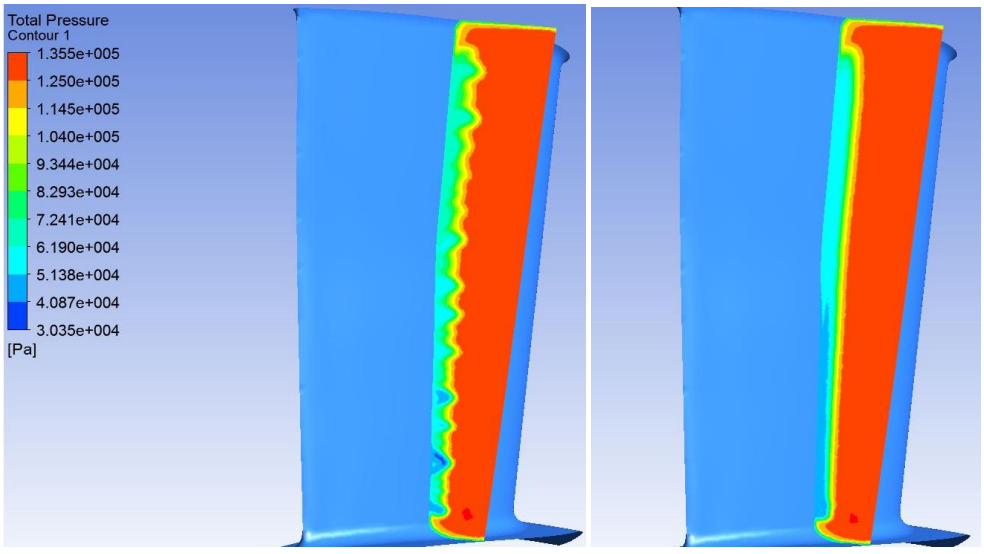

a. b.

Figura 6.7. Mean radius total pressure comparison in a downstream section for: a. $\boldsymbol{\tau = 53.6}$ % (53 sections) and b. $\boldsymbol{\tau = 75}$ % (70 sections) (42)

Injection system influence on different partial regimes

The cases presented above were reported at a partial load corresponding to an engine regime of approximately 89%. In order to determine the influence of the injection system on other loads, the performance of the turbine with and without injection was determined at other working regimes, lower and higher powers than the previous case. Using the turbine characteristic and the working line, the input parameters were determined for lower regimes, 84.5% and 80% respectively, and for higher regimes, 91% and 92.5% respectively.

In the case of lower power regimes compared to the reference regime, following the injection process, the turbine power increased by approximately 21-22%. Similarly, in the case of higher power regimes compared following the injection, the power generated by the turbine increases by about 25%. A comparison of regimens with and without injection is shown in Figure 6.8. It is thus observed that the performance of the turbine can be improved by using the injection system for different partial regimes. An greater influence with increasing regimes was also observed in this analysis, with the system having a more pronounced effect at higher partial regimes.

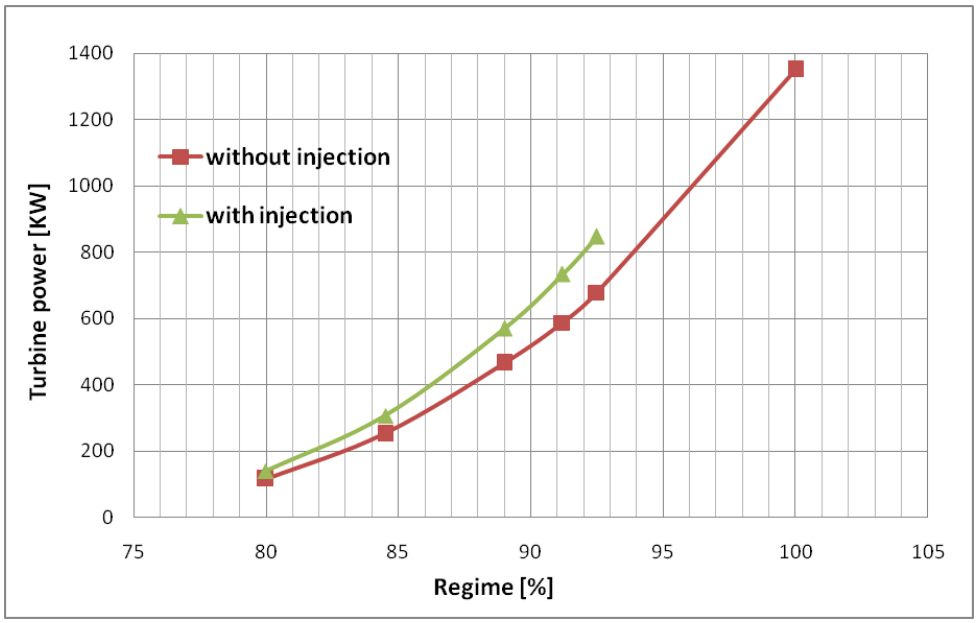

Figure 6.8. Turbine power comparison at different partial loads for the cases with and without injection (42)

Conclusion

To study the influence of the injection system on the flow through the turbine and on the performances, the influence of the injection diameter at different axial distances, as well as the influence of the number of orifices, was determined. It resulted that the power generated by the turbine can increase by more than 30% for certain cases, the best performance being obtained at small values of the injection diameter. Also, as it was demonstrated on the simplified 2D model, the influence of the axial distance shows a maximum around the value $Za \cong 0.27$.

In the case of the influence of the orifices number, an analysis was carried out for an injection diameter $Ø_{inj} = 0.6\,mm$, $Za = 0.2$ and a number of sections between 50 and 70. In this analysis, an increase in the power generated by the turbine was obtained by approximately 8% by increasing the number of orifices. A similar analysis was also carried out for an injection diameter $Ø_{inj} = 0.8\,mm$ and a number of sections between 30 and 40, resulting in an increase in the generated power of about 10%. To quantify this increase in injection area, a parameter called coverage degree was introduced. Thus, regardless of the injection diameter, an almost linear increase in the power generated by the turbine is obtained when the coverage degree increases. Power increases greater than 30% are achieved for high values of this parameter, >70%.

The injection system was also analyzed at other operating regimes compared to the previously defined reference one. Compared to this partial reference regime (89%), operating regimes of lower speed (80% and 84.5%) and higher speed (regime 91% and 93%) were analyzed. An increase in turbine generated power between 22% and 25% was achieved. An increase in the influence of the injection system was also determined as the operating regime increased.

CHAPTER 7 - VERIFICATION OF THE PERFORMANCE IMPROVEMENT METHOD OF AXIAL TURBINES AT PARTIAL REGIMES

For a verification of the results obtained for the reference turbine, an analysis was carried out to determine the influence of the injection system on the flow and performance for two axial turbines of different sizes.

Application of injection system for microturbine

The applied methodology is similar to the one used for the reference turbine, thus the 3D numerical model was created, the nominal point and the partial regime of interest were determined and the case with fluid injection was then calculated.

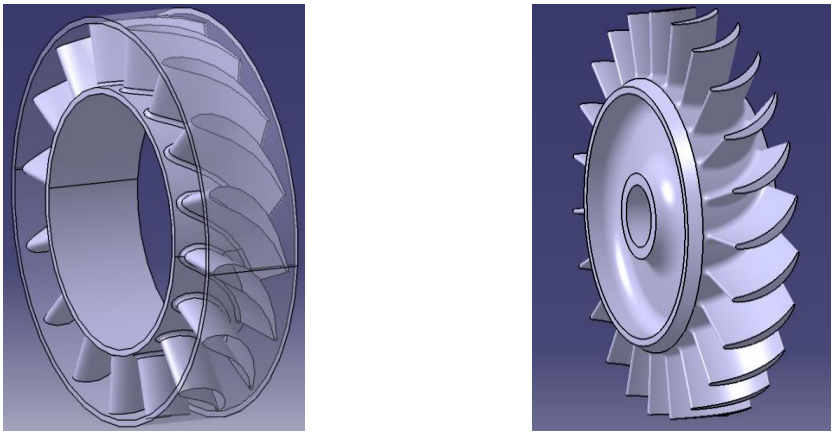

a. b.

Figure 7.1. Microturbine components: a.vane, b. rotor (43)

Similar to the reference turbine, 3D models were created and the numerical grid was generated. The numerical grid was established by determining its influence on turbine performance. For this unstructured numerical grid, the cells have an overall size of 0.5 mm, being crowded near the walls and near the injection holes.

The turbulence model and boundary conditions were set similar to the cases for the reference turbine. The injection system was generated according to the methodology presented previously, the 3D model being shown in Figure 7.2. For this microturbine, the flow through the turbine was studied at the nominal regime and at 5 partial loads representing regimes of 70%, 74%, 76%, 78% and 81% of the nominal speed. The parameters of the partial regimes were determined using the turbine characteristic and the operating line for the respective engine.

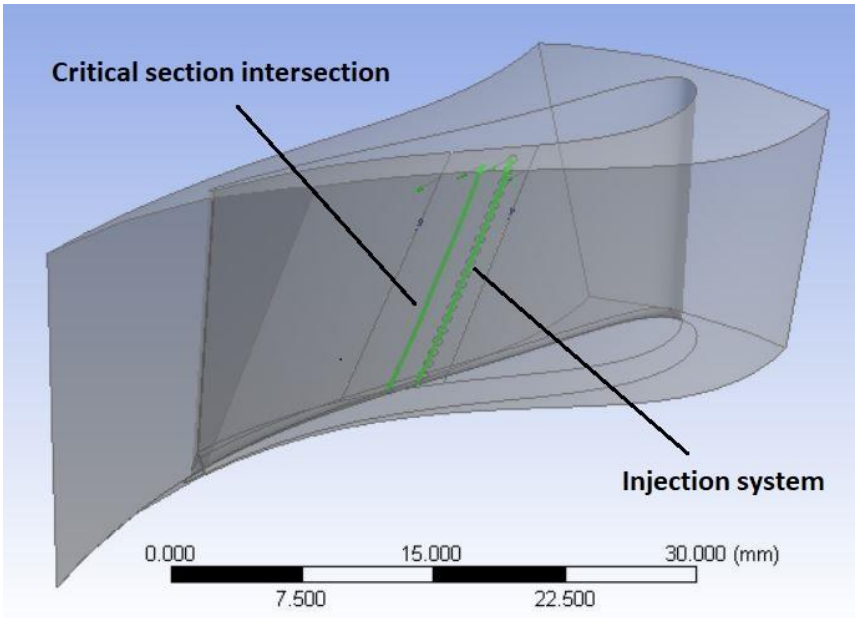

Figure 7.2. Fluid volume of the 3D model with injection system (43)

The injection process determined an increase in the power generated by the turbine by up to 21% depending on the partial regime at which the calculation was made. Similar to the partial regimes studied for the reference turbine, also in the case of the microturbine, an increase in the influence of the system can be noted with the increase of the operating regime. For the cases corresponding to regimes of 79% and 81% of the nominal speed, the increase in the power generated by the turbine after the injection process is lower due to the fact that for these regimes a flow of 2.5% of the working fluid flow could not be injected. This is due to blockage of fluid flow in the injection sections.

The comparison of the turbine power before and after the injection process is presented in Figure 7.3 which shows the power developed by the turbine for the operating regimes of the engine before the injection process according to the working line. An increase in the power slope developed following the injection process can be observed.

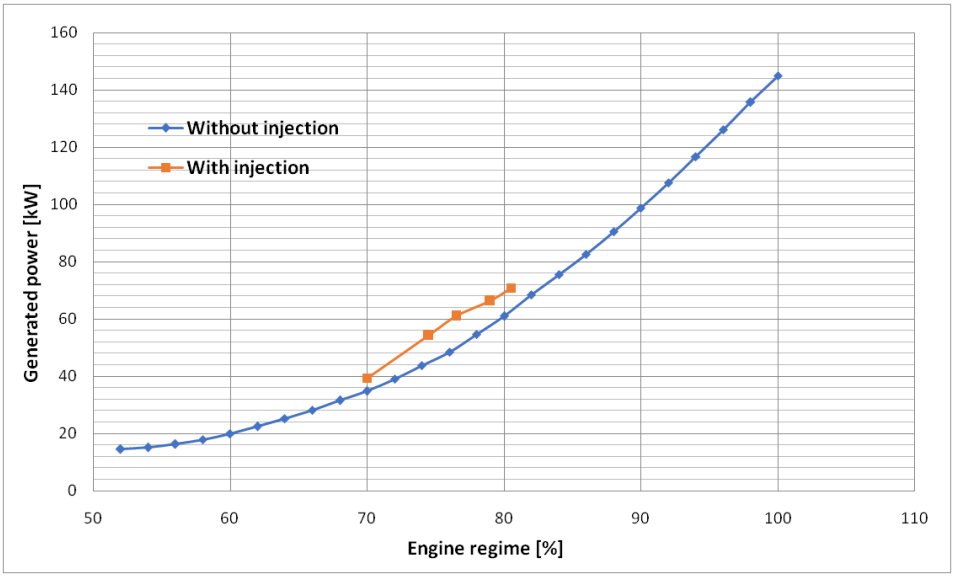

Figure 7.3. Turbine power generation before and after injection for different partial loads (43)

Similar to the results obtained in the case of the reference turbine, the working fluid is deviated from the suction side, which leads to the reduction of the flow section and implicitly to the acceleration of the fluid and the increase of the power developed by the microturbine. The reduction of the passage section can be seen in Figure 7.4 where the distribution of the total pressure at the vanes mean radius is shown.

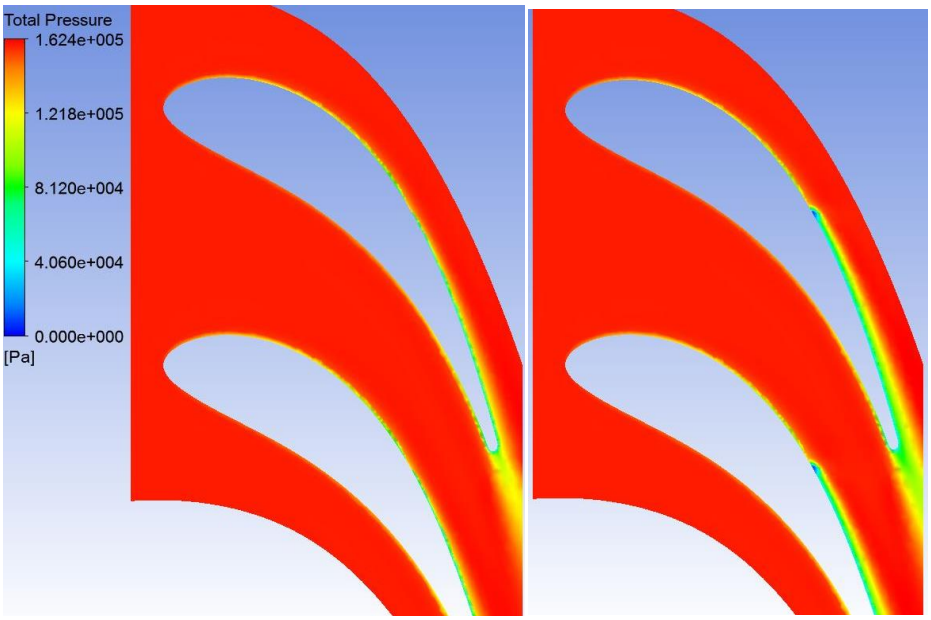

a. b.

Figure 7.4. Mean radius total pressure distribution for the case: a. without, b. with injection (43)

A verification of the previous results regarding the optimal injection position (Za) was carried out in the case of this microturbine. Thus, it resulted an increase in the influence of the injection system, from the point of view of the power generated by the turbine rotor when the

axial distance increases, reaching a maximum around the value Za≅0.28, followed by a decrease in the influence.

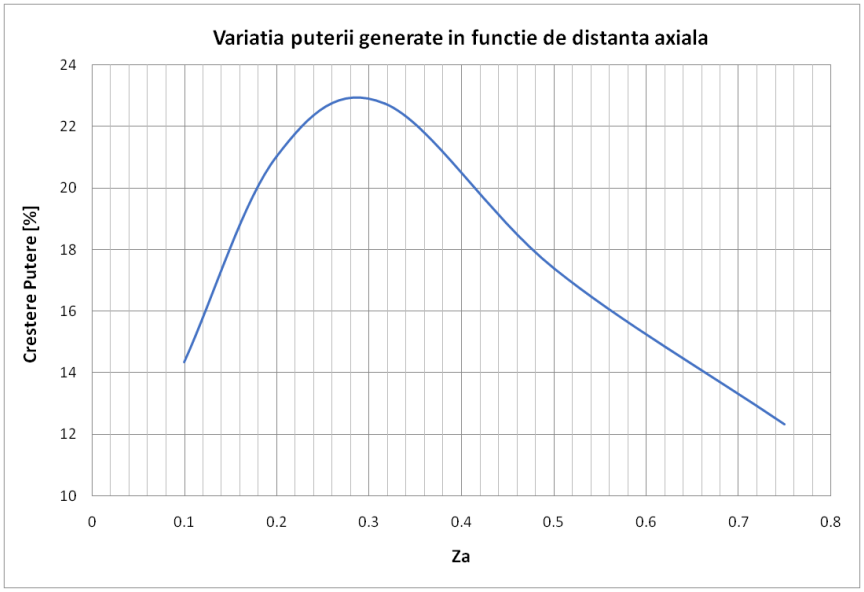

Figure 7.5. Injection system influence variation as a function of axial distance

Application of injection system for a small dimensions turbine

The injection system presented in this work was applied similar to the cases previously described for another small turbine whose geometry and performance are known. The turbine networks are shown in Figure 7.6.

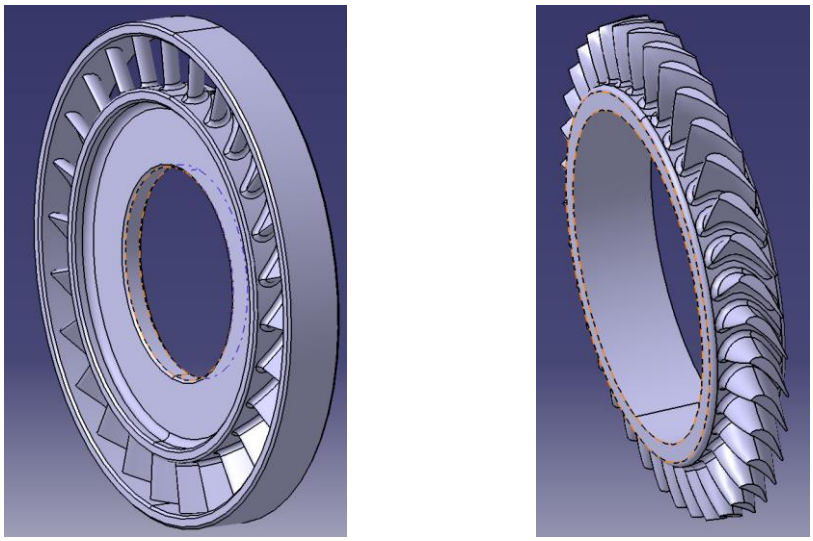

a. b.

Figure 7.6. Turbine components: a.vane, b. rotor

The injection system was generated according to the methodology presented previously, the 3D model being shown in Figure 7.7.

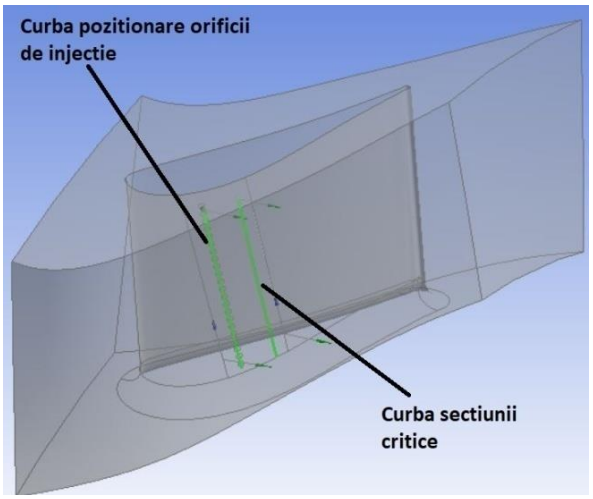

Figure 7.7. Fluid volume of the 3D model with injection system

The flow evolution through the vanes following the injection process is similar to the previous cases, with the diversion of the working fluid in the area of the orifices and the formation of a low pressure area downstream of the injection section followed by the attachment of the injection fluid to the suction side of the profile. Following the injection process, the turbine power increased by up to 21.5%. And in the case of this geometry, the increase in the influence of the injection system on the flow and implicitly on the performances is observed with the increase of the operating regime.

Graphically representing the regimes calculated before and after the injection according to the power generated, Figure 7.8, it can be observed, as in the previous cases, an increase in the slope of the power generation by the turbine at different regimes. Thus, higher powers can be achieved without changing the turbine input parameters. In this way, the engine speed can be increased without adding fuel.

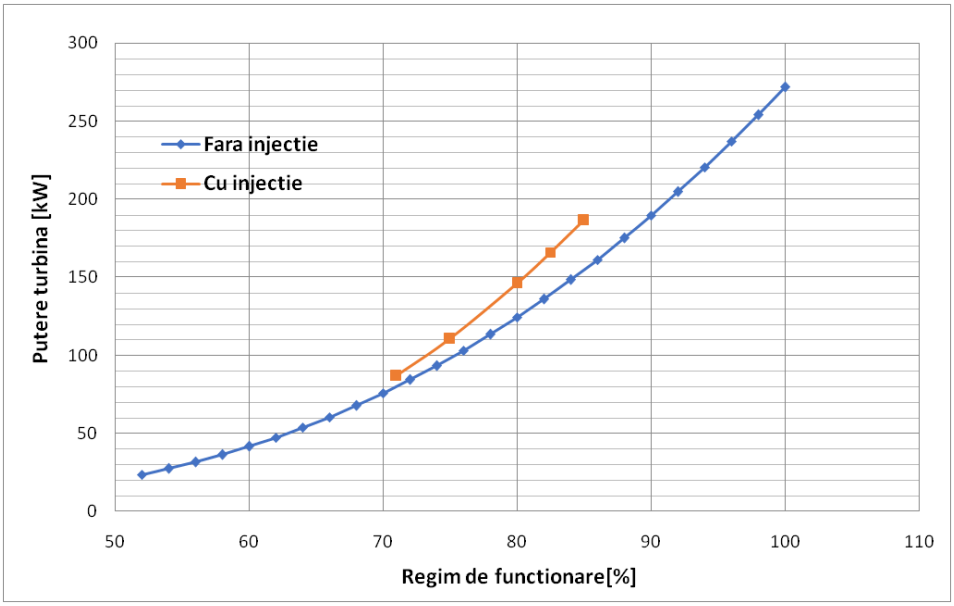

Figure 7.8. Turbine power generation before and after injection for different partial loads

Conclusion

For an additional validation of the results obtained in the case of the reference turbine, the injection system was also applied to two other axial turbines of different sizes (with power at the nominal regime of approximately 145 and 274 KW respectively). Thus, the geometries and parameters of the two turbines, the construction of the model and the analysis of the numerical grid were presented. In the case of the microturbine (nominal power of approximately 145 KW) 5 regimes between 70% and 81% were studied. The input data was set based on the working line and turbine characteristic. Increases in turbine generated power between 7.9% and 21% were achieved. Similar to the reference turbine, the influence of the injection system increases as the turbine ramps up.

In the case of the small turbine (nominal power of approximately 274 KW) 5 regimes between 71% and 85% were studied according to the working line of the respective engine. Increases in generated power between 10.5% and 21.5% were obtained, with a greater influence at higher regimes. In the case of the two studied turbines, similar to the reference turbine, by injecting the fluid into the channels, a diversion of the working fluid is achieved in the sense of reducing the passage section, which leads to its acceleration and implicitly to the increase of the power generated by the turbine. The diversion of the working fluid and the creation of a low pressure zone downstream of the injection section was indicated by the presentation of the total pressure and the absolute static pressure in the planes downstream of the injection section.

CHAPTER 8 - DETERMINING THE REACTION OF THE ENGINE ASSEMBLY TO THE ACTIVATION OF THE INJECTION SYSTEM

In previous chapters, the performance of the axial turbines at different regimes before and after the activation of the injection system was presented. The application of such a performance increase system in the assembly of an engine must also take into account the influence of the system on the other components. In order to determine the effect of the activation of the injection system on the gas turbine engine, a logical scheme was created to determine the response of the assembly to the imbalance created. Then, using a similar logic scheme, the fuel flow required to reach the initial speed is determined, before the injection system is activated.

Determination of the stabilized regime after activation of the injection system

When activating the performance increase system, the power developed by the respective turbine increases, as presented in the previous chapters, resulting in a surplus of power compared to the energy consumed by the compressor. This causes the respective rotor to accelerate and change the operating regimes for all engine components. In order to determine the variation of the engine parameters when the injection system is actuated, the logic diagram shown in Figure 8.1 was developed.

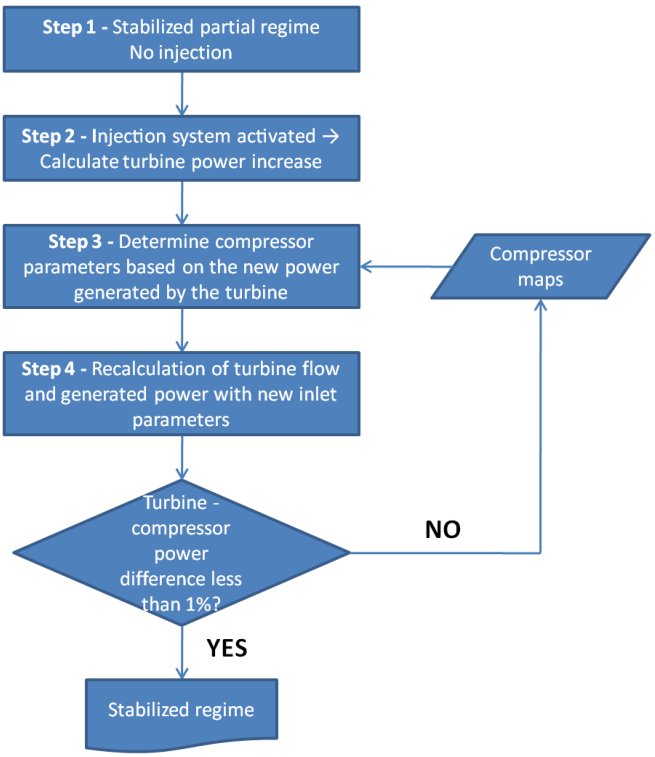

Figure 8.1. Logic scheme to identify the stabilized regime after injection process (43)

For this analysis, the microturbine presented in chapter 7.1 was used, it being part of the gas generator assembly of a microturbojet engine to drive a centrifugal compressor. The engine parameters at this stage are presented in Table 8.1

Table 8.1. – Engine parameters for the stabilized regime before injection (43)

Case	Regime [%]	Speed [rpm]	P_3^*[bar]	T_3^*[K]	$\dot{M}_3$ [kg/s]	T_2^*[K]	P_{inj}^*[bar]	T_{inj}^*[K]	Power difference ($W_T - W_C$) [KW]
Partial 2 before injection	74%	59200	2.47	820	0.39	395	N/A	N/A	0 (0%)

Activating the injection system requires extracting a flow of approximately 2.5% of the air flow. For this analysis, the bleed of the air at the exit from the compressor is considered; as a result the operation of the compressor (and implicitly the power consumed by it) is not affected. With the new turbine input data, the flow regime is recalculated by numerical simulation.

Table 8.2. – Engine parameters after injection (43)

Case	Regime [%]	Speed [rpm]	P_3^*[bar]	T_3^*[K]	$\dot{M}_3$ [kg/s]	T_2^*[K]	P_{inj}^*[bar]	T_{inj}^*[K]	Power difference ($W_T - W_C$) [KW]

Partial 2 after injection	74%	59200	2.47	831	0.39	395	1.71	395	10.2 (22.3%)

The surplus power generated by the turbine leads to the acceleration of the rotor, which determines another regime of the compressor. With the fuel flow rate held constant and the compressor output parameters determined based on the theoretical maps, the turbine inlet temperature is calculated and a new set of input parameters generated for the turbine numerical calculation. The compressor regime is determined in a first iteration based on the turbine power after injection and based on the theoretical characteristics and the working line. This completes step 3 of the logic scheme.

Table 8.3. – Engine parameters after acceleration determined by injection (43)

Case	**Regime [%]**	**Speed [rpm]**	$\mathbf{P_3^*[bar]}$	$\mathbf{T_3^*[K]}$	$\mathbf{\dot{M}_3\ [kg/s]}$	$\mathbf{T_2^*[K]}$	$\mathbf{P_{inj}^*[bar]}$	$\mathbf{T_{inj}^*[K]}$	**Power difference ($W_T - W_C$) [KW]**
New regime after acceleration	78%	62400	2.74	805	0.43	407	1.91	407	1.8 (3.1%)

Since for the new previously determined regime the turbine power is greater than the compressor power by about 3%, the rotor continues to accelerate. Thus, a new iteration is performed using a new point on the compressor map and recalculating the turbine inlet temperature. The new engine parameters resulting from the second iteration are presented in Table 8.4

Table 8.4.– Engine parameters after acceleration determined by injection, second iteration (43)

Case	**Regime [%]**	**Speed [rpm]**	$\mathbf{P_3^*[bar]}$	$\mathbf{T_3^*[K]}$	$\mathbf{\dot{M}_3\ [kg/s]}$	$\mathbf{T_2^*[K]}$	$\mathbf{P_{inj}^*[bar]}$	$\mathbf{T_{inj}^*[K]}$	**Power difference ($W_T - W_C$) [KW]**
New regime after acceleration second iteration	79%	63200	2.80	792	0.44	410	1.96	410	-0.3 (0.5%)

With the difference between the compressor and turbine powers of less than 1%, it is considered, for this study, that the engine has reached a stabilized regime. Even though the engine has reached a higher speed, the gains obtained are insignificant because the turbine has extracted more energy from the hot gas flow causing a lower temperature at the nozzle inlet which diminishes the effect of the increased air flow due to the acceleration of the compressor.

Determination of the initial regime by reducing the fuel flow

To determine the initial operating regime, the regime before the activation of the injection system, a logical process was created, similar to the one shown in Figure 8.1, where by the fuel flow is gradually decreased and the engine operating regime is approximated based on the theoretical maps, working line and the numerical calculation of the flow through the turbine. The iterative process is shown in Figure 8.2.

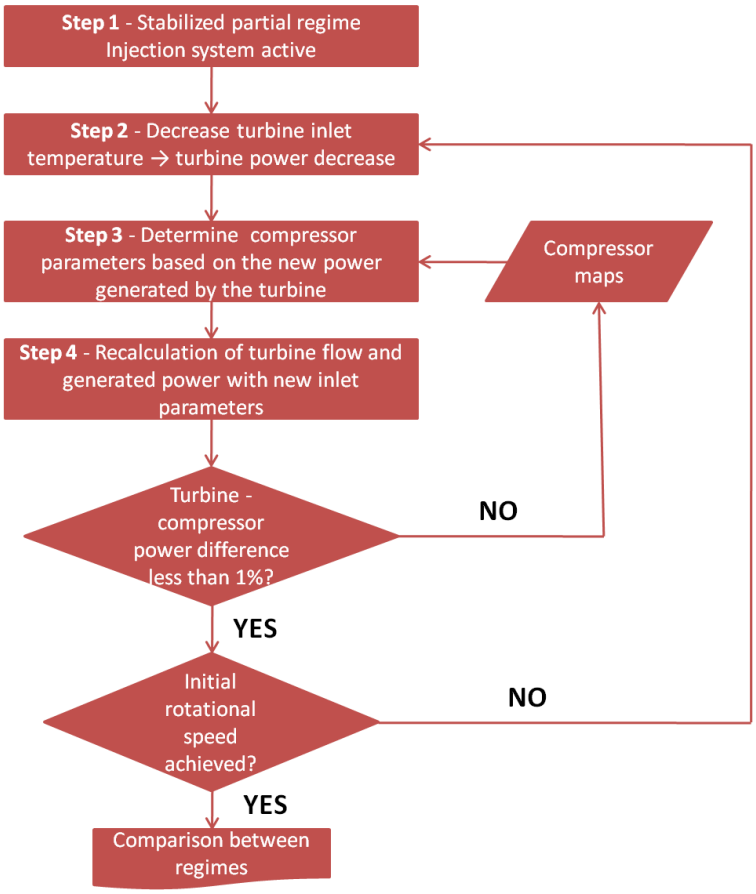

Figure 8.2. Logic scheme to identify the initial regime with the injection system active (43)

Starting from the stabilized regime reached after the injection, the engine parameters being present in Table 8.4, the turbine inlet temperature was decreased with an initial value of 20 degrees.

Table 8.5.– Engine parameters after turbine inlet temperature decrease (43)

Case	Regime [%]	Speed [rpm]	$P_3^*[bar]$	$T_3^*[K]$	$\dot{M}_3$ [kg/s]	$T_2^*[K]$	$P_{inj}^*[bar]$	$T_{inj}^*[K]$	Power difference ($W_T - W_C$) [KW]
Stabilized regime after turbine inlet temperature decrease	79%	63200	2.80	772	0.44	410	1.96	410	-8.2 (13.9%)

The power developed by the turbine following the drop in inlet temperature suggests an operating regime of 76%. Thus, the output parameters from the compressor are determined using the theoretical maps and the working line. With the new parameters at the exit from the compressor, the turbine inlet temperature is recalculated followed by the recalculation of the flow through the turbine. The results of this calculation are listed in Table 8.6.

Table 8.6.– Engine parameters after deceleration as a result of turbine inlet temperature decrease (43)

Case	Regime [%]	Speed [rpm]	$P_3^*[bar]$	$T_3^*[K]$	$\dot{M}_3$ [kg/s]	$T_2^*[K]$	$P_{inj}^*[bar]$	$T_{inj}^*[K]$	Power difference ($W_T - W_C$) [KW]
Regime after turbine inlet temperature decrease	76%	60800	2.60	803	0.412	401	1.82	401	-1.8 (3.6%)

With the turbine power less than the power consumed by the compressor, the engine speed continues to decrease, thus a new iteration is performed to determine the stabilized speed.

Table 8.7.– Engine parameters after deceleration, second iteration (43)

Case	Regime [%]	Speed [rpm]	$P_3^*[bar]$	$T_3^*[K]$	$\dot{M}_3$ [kg/s]	$T_2^*[K]$	$P_{inj}^*[bar]$	$T_{inj}^*[K]$	Power difference ($W_T - W_C$) [KW]

Stabilized regime after turbine inlet temperature decrease, second iteration	75%	60000	2.53	812	0.4	398	1.77	398	0.4 (0.8%)

Since the power difference between the two components is less than 1%, it is considered that the achieved regime is a stable one. However, the initial speed, 59200, was not reached, so the iterative process continues with a further decrease of the turbine inlet temperature, respectively of the fuel flow. The results of the second temperature drop are shown in Table 8.8.

Table 8.8.– Engine parameters after deceleration, second turbine inlet temperature decrease (43)

Case	**Regime [%]**	**Speed [rpm]**	$\mathbf{P_3^*[bar]}$	$\mathbf{T_3^*[K]}$	$\mathbf{\dot{M}_3\ [kg/s]}$	$\mathbf{T_2^*[K]}$	$\mathbf{P_{inj}^*[bar]}$	$\mathbf{T_{inj}^*[K]}$	**Power difference ($W_T - W_C$) [KW]**
Regime after second turbine inlet temperature decrease	75%	60000	2.53	810	0.4	398	1.77	398	-1.4 (2.9%)

After the temperature drops, a difference results between the power generated and the power consumed, thus the engine speed decreases.

Table 8.9.– Engine parameters after deceleration, second turbine inlet temperature decrease, second iteration (43)

Case	**Regime [%]**	**Speed [rpm]**	$\mathbf{P_3^*[bar]}$	$\mathbf{T_3^*[K]}$	$\mathbf{\dot{M}_3\ [kg/s]}$	$\mathbf{T_2^*[K]}$	$\mathbf{P_{inj}^*[bar]}$	$\mathbf{T_{inj}^*[K]}$	**Power difference ($W_T - W_C$) [KW]**
Stabilized regime after second turbine inlet	74%	59200	2.47	810	0.39	395	1.71	395	-0.2 (0.4%)

temperature decrease, second iteration									

After the second iterative deceleration process, the initial speed was reached, the regime being a stable one. Comparing the two regimes, the one before the injection system was activated and the one achieved after the system was activated and the fuel flow decreased resulted in a decrease of about 5% without significant variations in the thrust. Thus, the injection process causes a decrease in specific consumption.

Conclusion

The study presented in this chapter represents an initial estimate of the behaviour of the engine and its components when the injection system is activated. Even if the introduction of such a system for microturbines is not feasible, the technological complications being unjustified, in terms of the advantages of the system, the study represents a first analysis regarding the response of the gas turbine engine assembly to the activation of the injection system.

In the case of the power turbine discussed in the previous chapters the gains brought by the injection system were easy foreseen, an increase in the power of the turbine translates into an increase in power to the consumer or a reduction in the gas generator regime for the same power transmitted to the consumer, thus reducing fuel consumption. In the case of the turbines in the gas generator assembly, the injection system influences both the components downstream of the turbine and those upstream. The use of the injection system, in this case, leads to a better extraction of energy from the flow of hot gases reducing the energy available to the downstream components. Thus, the introduction of such a system must take into account the operating regimes of all the components involved, in some cases the gains may be insignificant.

CHAPTER 9 - FINAL CONCLUSIONS, ORIGINAL CONTRIBUTIONS AND FUTURE PERSPECTIVES

General conclusions

The present paper studies the performances of axial turbines and the variation of these performance at partial loads. Even though these systems achieve in modern engines high powers, efficiencies and reliability, these performance are achieved for a narrow range of operating conditions. With the departure from the nominal regime, the regime for which the respective turbine was designed, its performance drops sharply.

An analysis of the scientific literature in the field of axial turbines has identified empirical methods for determining the performance at partial regimes, but in terms of methods to reduce this shortcoming, no solution has been identified that can be applied to existing engines. Several solutions to adapt the flow regime through the channels to the turbine inlet conditions have been

identified, but these solutions are unusable because they affect the reliability of the engine or their impact is limited.

The paper presents the methods of calculating the performances of axial turbines, based on the velocity triangles, but also the calculation of losses based on empirical methods widely used in the industry. The decrease in the performance of axial turbines at partial regimes is caused by the change in the velocity triangles as a result of the change in the inlet conditions. Thus, in this paper, a method was proposed and analyzed to reduce these effects by improving the performances at partial regimes. By injecting a fluid at specific points of the vanes, the diversion of the working fluid and the reduction of the passage section through the vanes is followed. Thus, an acceleration of the working fluid at the exit from the vane is determined, which leads to an increase in the power developed by the turbine according to the Euler equation.

A research methodology was proposed in order to characterize the injection method, from the point of view of the influence on the turbine performance. A reference turbine, whose geometry is known, was thus selected and the flow through the respective channels was defined both at the nominal regime and at a partial regime by CFD numerical calculation.

The characterization of the injection system was carried out by determining the influence of various parameters, both geometric and gas-dynamic parameters. Through the variation of these parameters, a test matrix for the 2D model consisting of approximately 101 numerical cases was obtained. The results showed that fluid injection into the vanes causes the working fluid to deviate near the injection port and a low pressure zone appears. This area causes the cross section to decrease through the channels which leads to the acceleration of the working fluid. The previously described parameters influence the amplitude and positioning of this zone. In the case of the injection angle, it turned out that the perpendicular injection leads to the best results, the influence of the system decreasing linearly with the decrease of the injection angle. A similar effect was determined in the case of injected mass flow, with decreasing mass flow causing a decrease in system influence. An optimal position of the axial distance of the injection sections was identified. Thus, for a value of this parameter of about 0.27, the low pressure bubble is positioned in such a way that the maximum reduction of the minimum section of the vanes is obtained. Injection orifice sizes also have an influence on injection efficiency. The decrease in dimensions causes the injection speed to increase and the low pressure area to increase. Regarding the temperature of the injected fluid, the increase in temperature causes the increase of the injection speed and implicitly the influence of the system after a linear variation.

Based on the results obtained for the simplified model, the influence of different parameters was determined, such as: the sizes of the orifices, their number, but also the axial distance in order to verify the results obtained previously, for the three-dimensional model. The analysis of the results confirmed the existence of the optimal position for placing the injection sections on the suction side, at an axial distance of approximately 0.27. The results also showed that the influence of the injection system on the flow through the channels and on the performance of the turbine is greater when using a large number of injection sections with the smallest possible dimensions. Thus, in order to quantify both the effect of the orifice sizes and their number, a new parameter called coverage degree was defined. The representation of the

results according to this parameter showed that the influence of the system increases linearly with the increase of this parameter, increases of the power generated by the turbine rotor >30% can be achieved for a coverage degree >70%.

In order to determine the efficiency of the injection system according to the operating regime, the performance of the turbine was calculated, before and after the injection, for a number of 5 partial regimes. From this analysis it emerged that the effect of the system is not limited to a single partial regime and that it can be used over a wide range of regimes. It also resulted that the influence of the system on the performance of the turbine increases with the increase of the operating regime, the power of the turbine increasing, following the injection process by 21% to 25% depending on the studied regime.

The injection system has also been applied to other axial turbines of different sizes. Two axial turbines, single-stage, with nominal powers of approximately 150 and 280 kW were chosen for this study. In both cases, the construction of the numerical model was presented, the injection system being applied for 5 partial regimes for each turbine. It resulted, as in the case of the reference turbine, that the system produces the deflection of the working fluid near the minimum section of the vanes, leading to the acceleration of the working fluid and implicitly to the increase of the power generated by the rotor. The conclusion determined in previous cases regarding the existence of an optimal position of the injection sections was also verified. The analysis confirmed the previously determined results, identifying an optimal position at an axial distance of approximately 0.28. In the case of the two turbines studied, as in the case of the reference turbine, it turned out that the injection system has a stronger influence at higher regimes, with 21% increases in generated power being achieved depending on the regime studied, for both turbines.

The implementation of such a performance increase system is a complex process that requires knowledge of the characteristics and operation mode of the respective engine and its components. In this sense, a study was conducted to determine the response of the engine assembly and its components when the injection system is activated in the case of a turbine in a gas generator assembly. The analysis was based on a logical scheme for iterative calculation of the power generated by the turbine after injection and the regimes reached by the compressor as a result of the increased power. If the fluid injection has caused a significant increase in engine regime and speed, the benefits of this increase are limited due to the fact that the injection has resulted in a better extraction of mechanical energy from the potential energy of the combustion gases by the turbine. In this way, the energy available to the exhaust nozzle decreases, thus diminishing the effect of the increase in air flow as a result of the acceleration of the compressor. A logical scheme was also introduced to decrease the regime reached after the injection process in order to reach the initial speed. The iterative process is based on the calculation of the power generated by the turbine and the resulting compressor speed as the fuel flow decreases. The analysis showed that the same operating regime can be achieved with a decrease in fuel consumption of about 5% without noticeable changes in traction force, thus improving the specific consumption of the respective engine.

Personal contributions

Contributions were made by proposing a new method of increasing performance, characterizing that method and determining the influence of different parameters as well as determining the influence on the components and the engine in general. The proposed system has no moving elements in its composition, being suitable to the operating conditions specific to modern engines, reaching, depending on the configuration of the system, increases in the generated power of over 30%. Thus, contributions are made in terms of improving the performance of axial turbines and engines operating at partial regimes. This helps to reduce fuel consumption, emissions and greenhouse gases. Also, the work contributes to widening the range of applicability of gas turbine engines as a result of the increase in performance at low regimes.

The work also contributes to the identification of the influence of various parameters, both geometric and gas-dynamic, on the performance of the turbine, generating a set of numerical data and variation trends for a series of analyzed parameters. The studies carried out in this work led to the identification of an optimal position of the injection sections on the suction side of the vanes. The influence of the injection system is maximum, for the respective conditions, if the injection is carried out at a value of the axial distance of approximately 0.27. The influence of the system on different partial regimes was also determined, demonstrating that the system can be applied over a wide range of regimes. Thus, it turned out that the injection system has a greater influence at higher regimes.

The work also contributes to the verification of the proposed method for different turbine geometries. In this sense, it has been demonstrated that the system can be applied, with similar results, for turbines of different sizes over a wide range of operating regimes. Studies have shown, as in the previous case, that the system has a more pronounced influence at high regimes.

Also, the work contributes to determining the influence of such a method on the operation of engines for which this system is active. In this sense, a logical calculation scheme was introduced and an analysis was conducted to determine the response of the engine assembly and its components to the activation of the injection system.

Future research directions

The experimental validation of the results obtained in this thesis represents the main direction of future research. Reproducing the conditions used in the studies presented above is a complex process, requiring dedicated experimental stands, complex measurement techniques and specific instrumentation.

An optimization of the injection system can be achieved by using different injection section configurations. The positioning of the orifices along two or more lines on the radial direction of the suction side of the vanes can lead to the increase of the distance between the orifices thus simplifying the manufacturing process without significantly diminishing the influence of the system. System optimization can also be achieved by using a pulsating injection system.

The introduction of an empirical method to calculate the influence of the injection system represents another important future research direction. Based on the results obtained in this thesis, regarding the influence of various parameters on the influence of the system, empirical correction factors can be determined for the calibration of a simplified analytical method. The introduction of such a method would lead to a simplification of the procedure and calculation time for various configurations of the injection system.

Another research direction in the future is the study of the flow through the injection channels. In this sense, the studies must focus on the determination of pressure losses, heat transfer and the internal geometries of the injection channels.

Also, the present study was based on a simple turbine geometry without complex cooling systems. The interaction of the injection system with the vane cooling systems represents another future research direction. The interaction of the two systems is a complex process requiring a large computing power and special attention to the numerical model.

CHAPTER 10 - BIBLIOGRAPHY

1. **Boyce, Meherwan P.** *Gas Turbine Engineering Handbook.* s.l. : Elsevier Science, 2011. 0123838436.
2. **Sumanta Acharya, Yousef Kanani,.** Chapter Three - Advances in Film Cooling Heat Transfer. [autorul cărții] John P. Abraham, John M. Gorman Ephraim M. Sparrow. *Advances in Heat Transfer.* s.l. : Elsevier, 2017.
3. *CFD Analysis for Axial Turbine Performance Maps Estimation.* **Razvan Nicoara, Daniel Olaru.** 1, Bucharest : TURBO Scientific Journal, 2019, Vol. 6.
4. *Axial Turbine Performance Estimation During Dynamic Operations.* **Razvan Nicoara, Valeriu Vilag, Jeni Vilag, Zoltan Kolozvary.** 2, s.l. : International Journal of Aeronautical and Space Sciences, 2021, Vol. 22. https://doi.org/10.1007/s42405-020-00312-4.
5. **D.G. Ainley, G.C.R. Mathieson.** *A method of performance estimation for axial-flow turbines.* London : AERONAUTICAL RESEARCH COUNCIL REPORTS AND MEMORANDA, 1951.
6. *Improvements to the Ainley-Mathieson Method of Turbine Performance Prediction.* **Dunham, J., and Came, P. M.** 3, s.l. : ASME Journal of Engineering for Power, 1970, Vol. 92.
7. *Off-Design Flow Analysis and Performance Prediction of Axial Turbines.* **Milan Petrovic, Walter Riess.** Orlando, Florida, USA : Proceedings of the ASME 1997 International Gas Turbine and Aeroengine Congress and Exhibition. Volume 1: Aircraft Engine; Marine; Turbomachinery; Microturbines and Small Turbomachinery, 1997. https://doi.org/10.1115/97-GT-055.
8. **Clarence Edgar Le Bell, Alvin Taub.** *VARIABLE STATOR WANES. 3237918* Washington, D.C, SUA, 30 August 1966.
9. **Wang, Yang.** Study of Power Minimization of Co-Flow Jet Active Flow Control with Fixed Airfoil Geometry. *Master's thesis.* Miami, SUA : University of Miami, 2019.
10. *Aerodynamic Performance Analysis of Co-Flow Jet Airfoil.* **C M Vigneswaran, Vishnu Kuma.** 1, s.l. : International Journal of Aviation, Aeronautics, and Aerospace, 2021, Vol. 8.
11. *Aerodynamic performance enhancement of co-flow jet airfoil with simple high-lift device.* **Haolin Zhi, Zhenhao Zhu, Yujin Lu, Shuanghou Deng, Tianhang Xiao.** 9, s.l. : Chinese Journal of Aeronautics, 2021, Vol. 34.

12. *A Novel Airfoil Circulation Augment Flow Control Method Using Co-Flow Jet.* **Gecheng Zha, Craig Paxton.** s.l. : AIAA, 2004. DOI: 10.2514/6.2004-2208.
13. *Velocity Field for an Airfoil with Co-Flow Jet Flow Control.* **AAdam Wells, Clark Conley, Bruce Carroll, Craig Paxton, Gecheng Zha.** s.l. : 44th AIAA Aerospace Sciences Meeting and Exhibit, 2006. DOI: 10.2514/6.2006.
14. *Effects of CoFlow-Jet Active Flow Control on Airfoil Stall.* **Shima Yazdani, Erfan Salimipour, Ayoob Salimipour, Mikhail Sheremet, Mohammad Ghalambaz.** 6, s.l. : International Journal of Numerical Methods for Heat & Fluid Flow, 2023, Vol. 33. https://doi.org/10.1108/HFF-04-2022-0219.
15. *Separation Control on a Very High Lift Low Pressure Turbine Airfoil Using Pulsed Vortex Generator Jets.* **Ralph Volino, Mounir Ibrahim.** s.l. : Applied Thermal Engineering, 2012, Vol. 49. https://doi.org/10.1016/j.applthermaleng.2011.08.028.
16. **McQuilling, Mark.** Experimental Study Of Active Separation Flow Control In A Low Pressure Turbine Blade Cascade Model. *Master's Thesis.* Lexington, Kentucky, SUA : University of Kentucky, 2004.
17. *Turbine blade boundary layer separation suppression via synthetic jet: An experimental and numerical study.* **hiara Bernardini, Mauro Carnevale, Madhab Manna, Francesco Martelli, Daniele Simoni, Pietro Zunino.** s.l. : Journal of Thermal Science, 2012, Vol. 21. https://doi.org/10.1007/s11630-012-0561-2.
18. *Separation and Transition Control on an Aft-Loaded Ultra-High-Lift LP Turbine Blade at Low Reynolds Numbers: Low-Speed Investigation.* **Xue Zhang, Maria Vera-Morales, Howard Hodson, Neil Harvey.** 3, s.l. : Journal of Turbomachi-nery-transactions of The Asme, 2006, Vol. 128. https://doi.org/10.1115/1.2187524.
19. *Validation of RANS-Modelling Approaches for Active Flow Control by Vortex Generating Jets in a Low-Pressure Turbine Cascade.* **Florian Herbst, Marc Biester, Andreas Fiala, Karl Engel, Joerg Seume.** Marseille, France : Proceedings of 8th International Symposium on Engineering Turbulence Modelling and Measurements – ETMM8, 2010.
20. *A numerical study of active flow control for low pressure turbine blades.* **Christian Rohr, Zhiyin Yang.** Xian, China : Proceedings of 4th International Symposium on Jet Propulsion and Power Engineering, 2012.
21. *Numerical Investigation of Active Flow Control for Low-Pressure Turbine Blade Separation.* **Dieter Postl, Andreas Gross, H. Fasel.** Reno, Nevada : 42nd AIAA Aerospace Sciences Meeting and Exhibit, 2004. https://doi.org/10.2514/6.2004-750.
22. *Numerical Simulation of a Low Pressure Turbine Blade Employing Active Flow Control.* **Marshall Galbraith, Amit Kasliwal, Kirti Ghia, Urmila Ghia.** Miami, Florida, USA : Proceedings of the ASME 2006 2nd Joint U.S.-European Fluids Engineering Summer Meeting Collocated With the 14th International Conference on Nuclear Engineering, 2006. https://doi.org/10.1115/FEDSM2006-98566.
23. *Simulation of Active Flow Control for a Low Pressure Turbine Blade Cascade.* **Andreas Gross, H. Fasel.** Reno, Nevada : 43rd AIAA Aerospace Sciences Meeting and Exhibit, 2005. https://doi.org/10.2514/6.2005-869.
24. *Active Flow Control of Low-Pressure Turbine Separation.* **Wolfgang Balzer, Andreas Gross, H. Fasel.** Pittsburgh, PA, USA : DoD High Performance Computing Modernization Program Users Group Conference, 2007. doi: 10.1109/HPCMP-UGC.2007.8..
25. *Transient Performance of Separated Flows: Characterization and Active Flow Control.* **Jorge Saavedra, Guillermo Paniagua.** 1, s.l. : Journal of Engineering for Gas Turbines and Power, 2018, Vol. 141. https://doi.org/10.1115/1.4040685.

26. *Experimental analysis of Reynolds effect on flow detachment and sudden flow.* **Saavedra, J (Saavedra, Jorge) și Paniagua, G.** s.l. : EXPERIMENTAL THERMAL AND FLUID SCIENCE, Vol. 126. DOI: 10.1016/j.expthermflusci.2021.110398.
27. *Response of Separated Boundary Layers to Steady and Pulsated Flow Injection. Journal of Turbomachinery.* **Hunter Nowak, Federico Rodríguez, Iman Rahbari, John Clark, Guillermo Paniagua.** 6, s.l. : Journal of Turbomachinery, 2022, Vol. 145. https://doi.org/10.1115/1.4056184.
28. *Stability-analysis-based optimization to control flow separation over a diffusing.* **Wang, YZ (Wang, Yinzhu), Ferrer, E (Ferrer, Esteban) și Saavedra, J.** 1, s.l. : PHYSICS OF FLUIDS, Vol. 33. DOI: 10.1063/5.0034892.
29. *Analysis of the boundary layer stability to assess flow separation control capability in.* **Padilla Montero, Iván &amp, Saavedra, Jorge &amp și Paniagua.** Glasgow, UK : 7th European Conference on Computational Fluid, 2018.
30. *Optimization of the base bleed to control trailing edge flows in a wide range of Mach.* **Martinez-Cava, Alejandro & Valero, Eusebio & Saavedra, Jorge & Lozano, Francisco & Paniagua, Guillermo.** Madrid, Spain : 8th European Conference For Aeronautics And Aerospace Sciences (EUCASS), 2019.
31. *urbine blade boundary layer separation suppression via synthetic jet: An experimental and numerical study.* **Chiara Bernardini, Mauro Carnevale,Madhab Manna, Francesco Martelli, Daniele Simoni, Pietro Zunino.** s.l. : Journal of Thermal Science, 2012.
32. *Application and Improvement of Gas Turbine Blades Film Cooling.* **Koval, Svetlana.** Singapore : International Conference on Aerospace System Science and Engineering, 2018.
33. *Film cooling of cylindrical holes on turbine blade suction side near leading edge.* **Zhiyu Zhou, Haiwang Li, Haichao Wang, Gang Xie, Ruquan You.** s.l. : International Journal of Heat and Mass Transfer, 2019, Vol. 141.
34. *Scaling criteria accuracy for turbine blade film cooling effectiveness at unmatched temperature ratio conditions.* **Weicheng Zhao, Zhongran Chi, Shusheng Zang.** s.l. : Applied Thermal Engineering, 2021, Vol. 197.
35. *Enhancing film cooling effectiveness in a gas turbine end-wall with a passive semi cylindrical trench.* **Ravi Duraisamy, Parammasivam Mahali.** 3, s.l. : Thermal Science, 2019, Vol. 23.
36. *Numerical and experimental investigation of turbine blade film cooling.* **Amar Berkache, Dizene Rabah.** s.l. : Heat and Mass Transfer, 2017, Vol. 53.
37. *Cooling and Capability Analysis Methodology: Towards Development of a Cost Model for Turbine Blades Film Cooling Holes.* **Javier Continente, Essam Shehab, Konstantinos Salonitis, Sree Tammineni, Phani Chinchapatnam.** TU Delft, Delft, Netherlands : Proceedings of The 22nd ISPE Conference on Concurrent Engineering, 2015.
38. *Conjugate calculation of a film-cooled blade for improvement of the leading edge cooling configuration.* **Norbert Moritz, Karsten Kusterer, Dieter Bohn, Takao Sugimoto, Ryozo Tanaka, Tomoki Taniguchi.** s.l. : Propulsion and Power Research, 2013.
39. **S.L. Dixon, C.A. Hall.** *Fluid Mechanics and Thermodynamics of Turbomachinery 7th edition.* USA : Elsevier Inc., 2014.
40. *A Procedure for Estimating Losses in the Flow Path of Axial Turbines in Calculating Their Characteristics.* **M. Kh. Mukhtarov, V. I. Krichakin.** s.l. : Teploenergetika, 1969, Vol. 7.
41. *Numerical Study Of Axial Turbines Performance En-hancement Technique By Specific Fluid Injection.* **Razvan Nicoara, Daniel Crunteanu, Valeriu Vilag.** 3, Bucharest : U.P.B. Scientific Bulletin Series D, 2022, Vol. 83.

42. *Axial Turbine Performance Enhancement by Specific Fluid Injection.* **Razvan Nicoara, Daniel Crunteanu, Valeriu Vilag.** 47, s.l. : Aerospace, 2023, Vol. 10. https://doi.org/10.3390/aerospace10010047.
43. *Application of a Performance-Improvement Method for Small-Size Axial Flow Turbines.* **Razvan Nicoara, Daniel Crunteanu, Valeriu Vilag.** 928, s.l. : Aerospace, 2023, Vol. 10. https://doi.org/10.3390/aerospace10110928.